Figure 1. Synthetic scheme of IBD monomer **8**

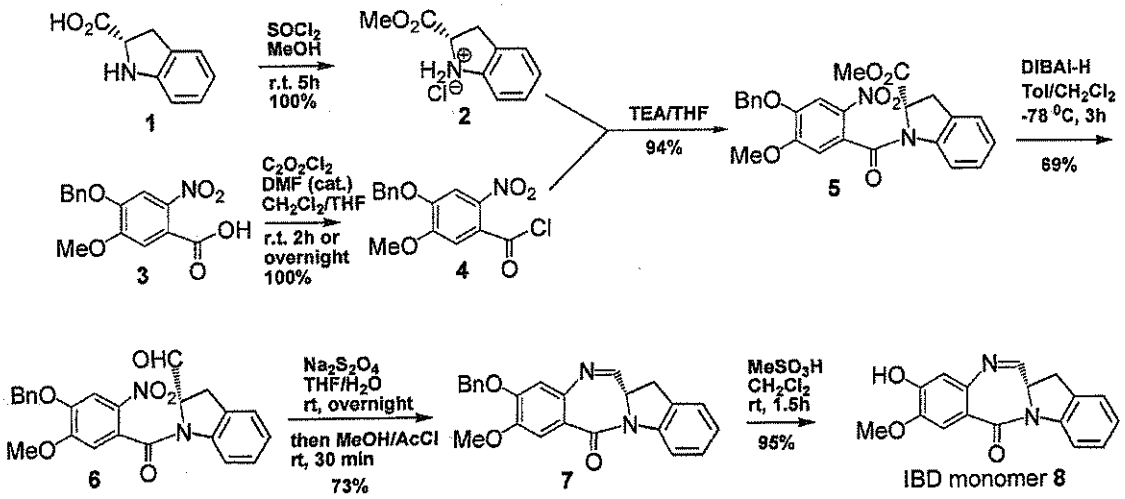


Figure 2. Synthetic scheme of OBD monomer **14**

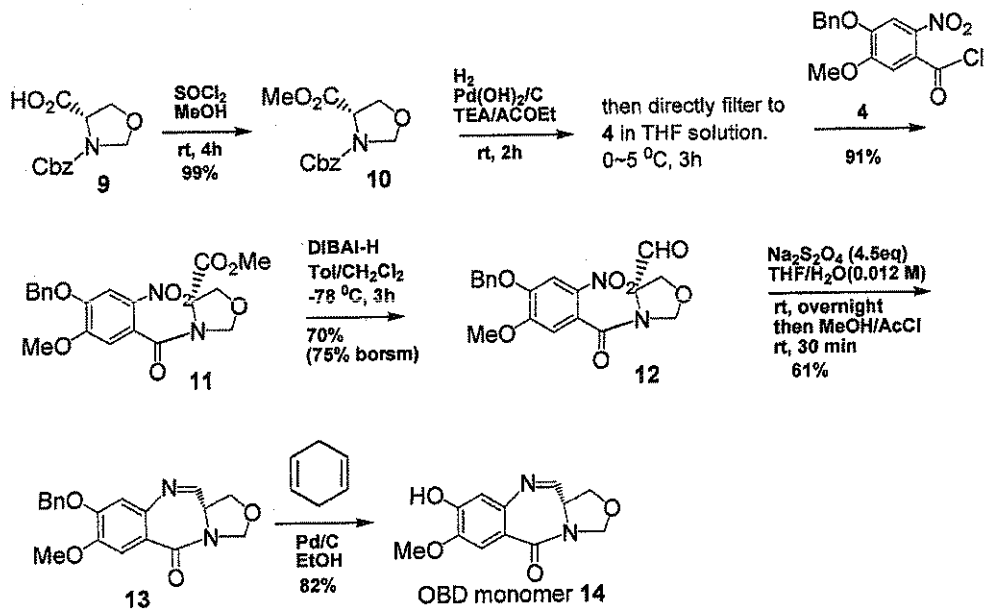


Figure 3. Synthetic scheme of dimer **15 (IGN-09)**

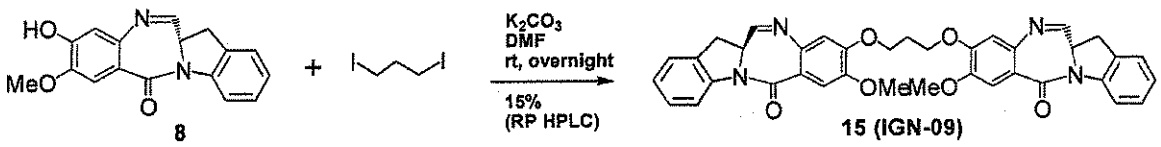


Figure 4. Synthetic scheme of dimer **18 (IGN-01)**

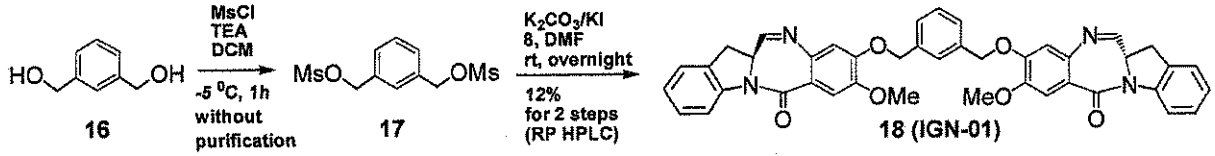


Figure 5. Synthetic scheme of dimer **19 (IGN-02)**

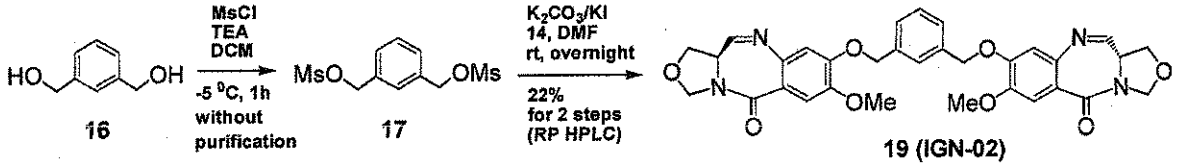


Figure 6. Synthetic scheme of the linkers

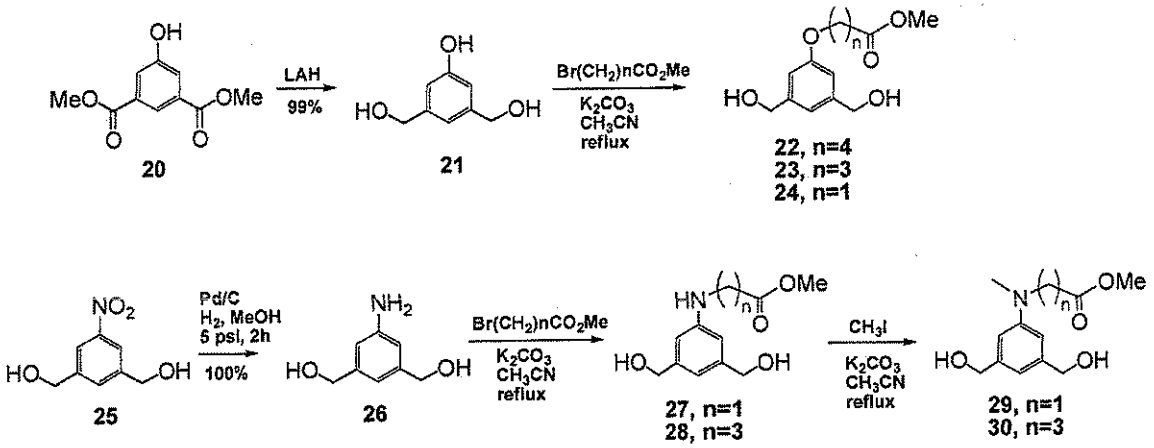


Figure 7. Synthetic scheme of dimers **34**, **35**, **36**, **39** and **40** (**IGN-03~07**)

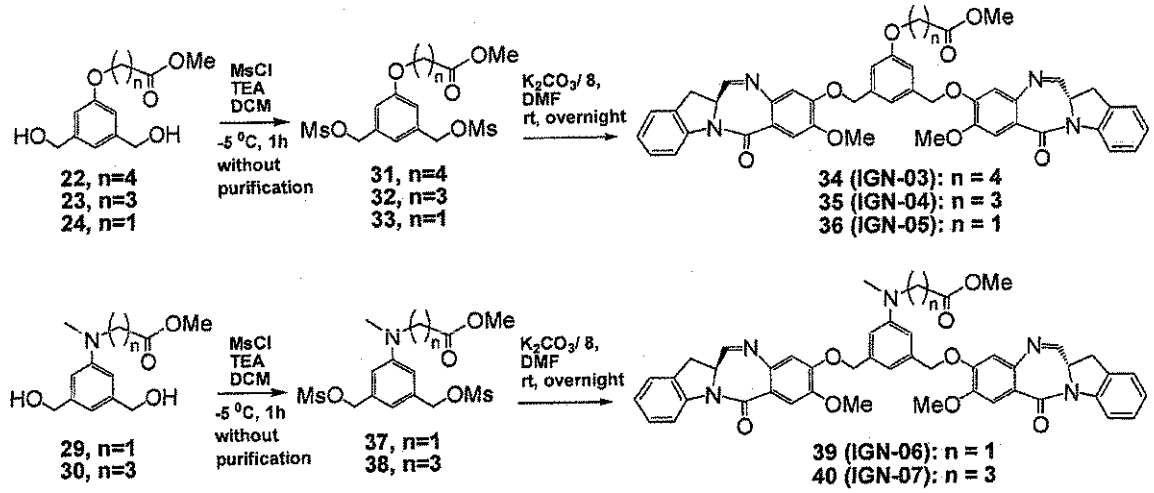


Figure 8. Synthetic scheme of the NHS esters **43**, **44** and **46**

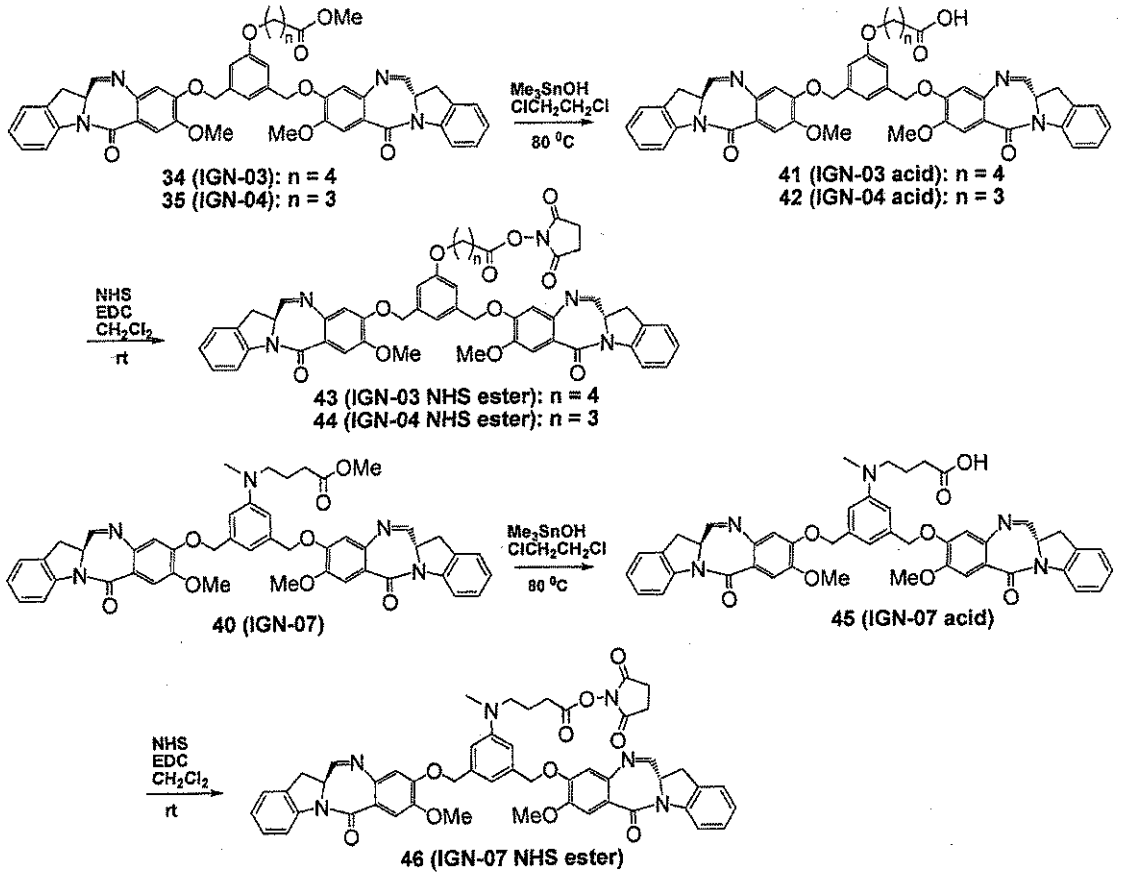


Figure 9. Synthetic scheme of thiol **49**

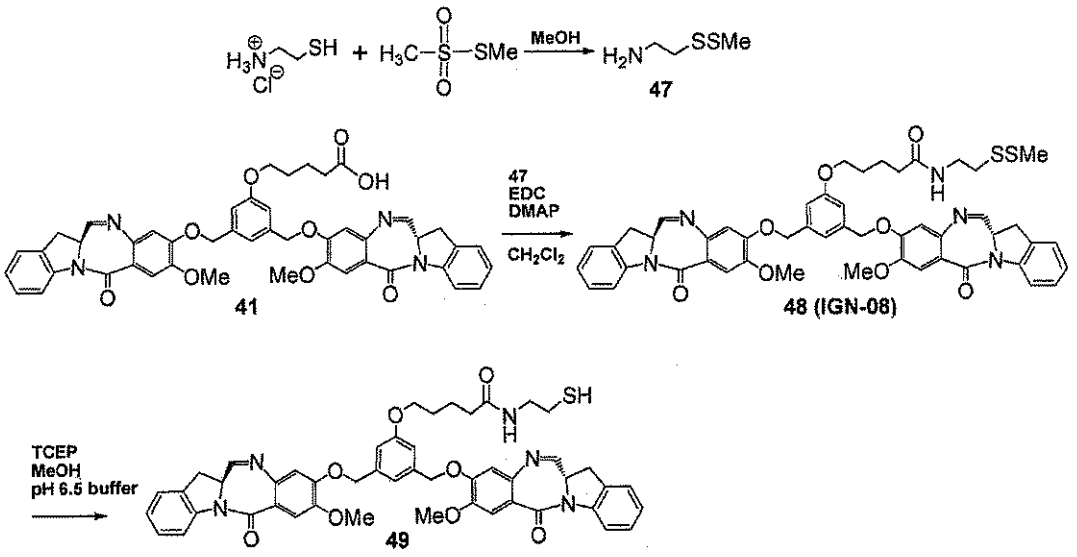


Figure 10. Synthetic scheme of disulfide **51**

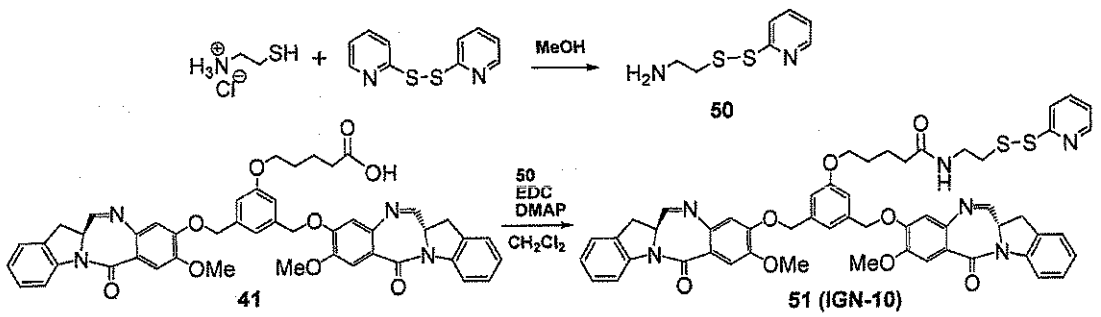


Figure 11. Synthetic scheme of B-ring modified monomer **58**

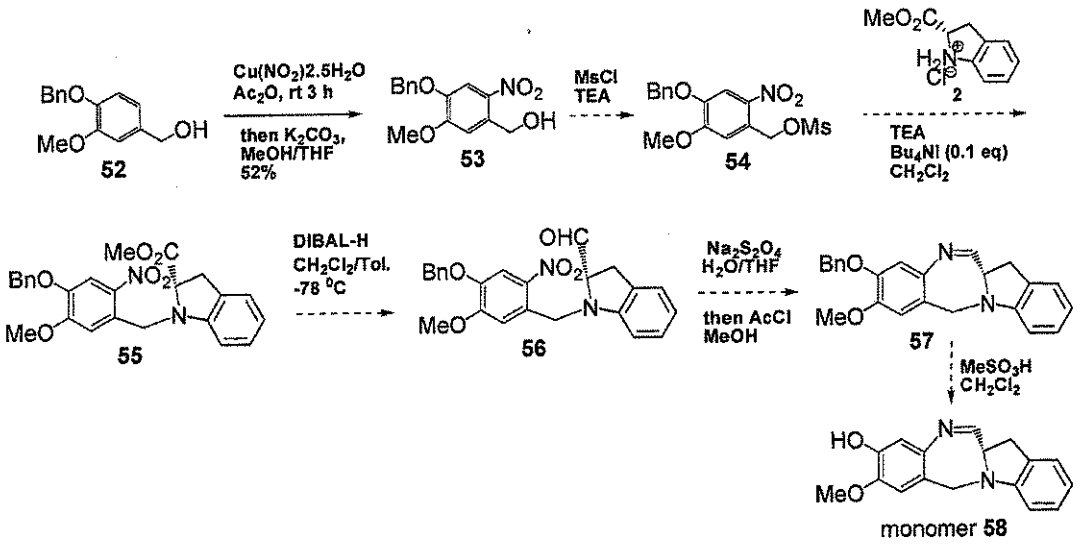


Figure 12. Synthetic scheme of isoindolinobenzodiazepine monomer **66**

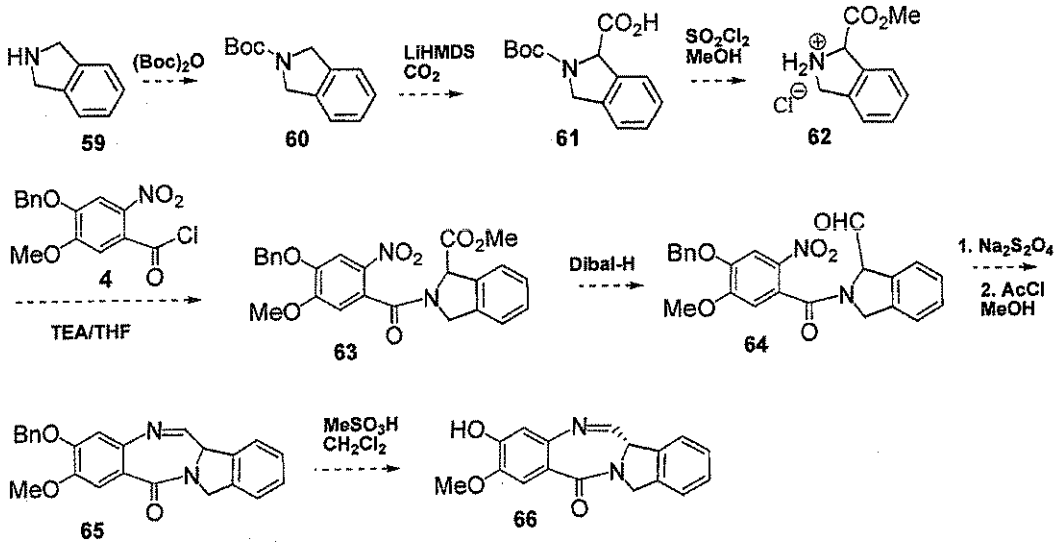


Figure 13. Synthetic scheme of compound **82** with linker attached to the Indoline moiety

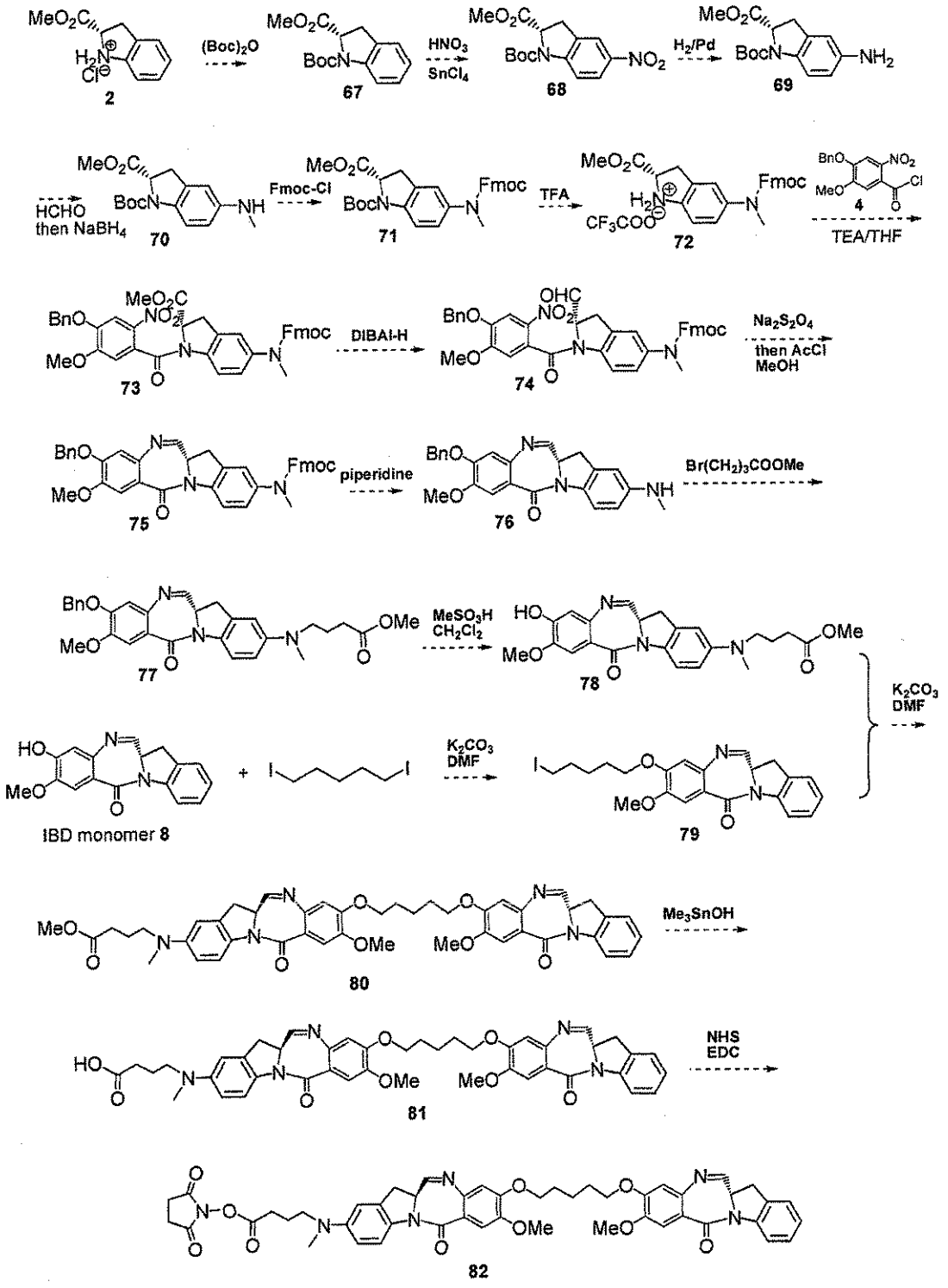


Figure 14. Synthetic schemes of dimers **87**, **88**, **92**, **96** and **100** containing $(PEG)_n$ moiety on the linear linkers

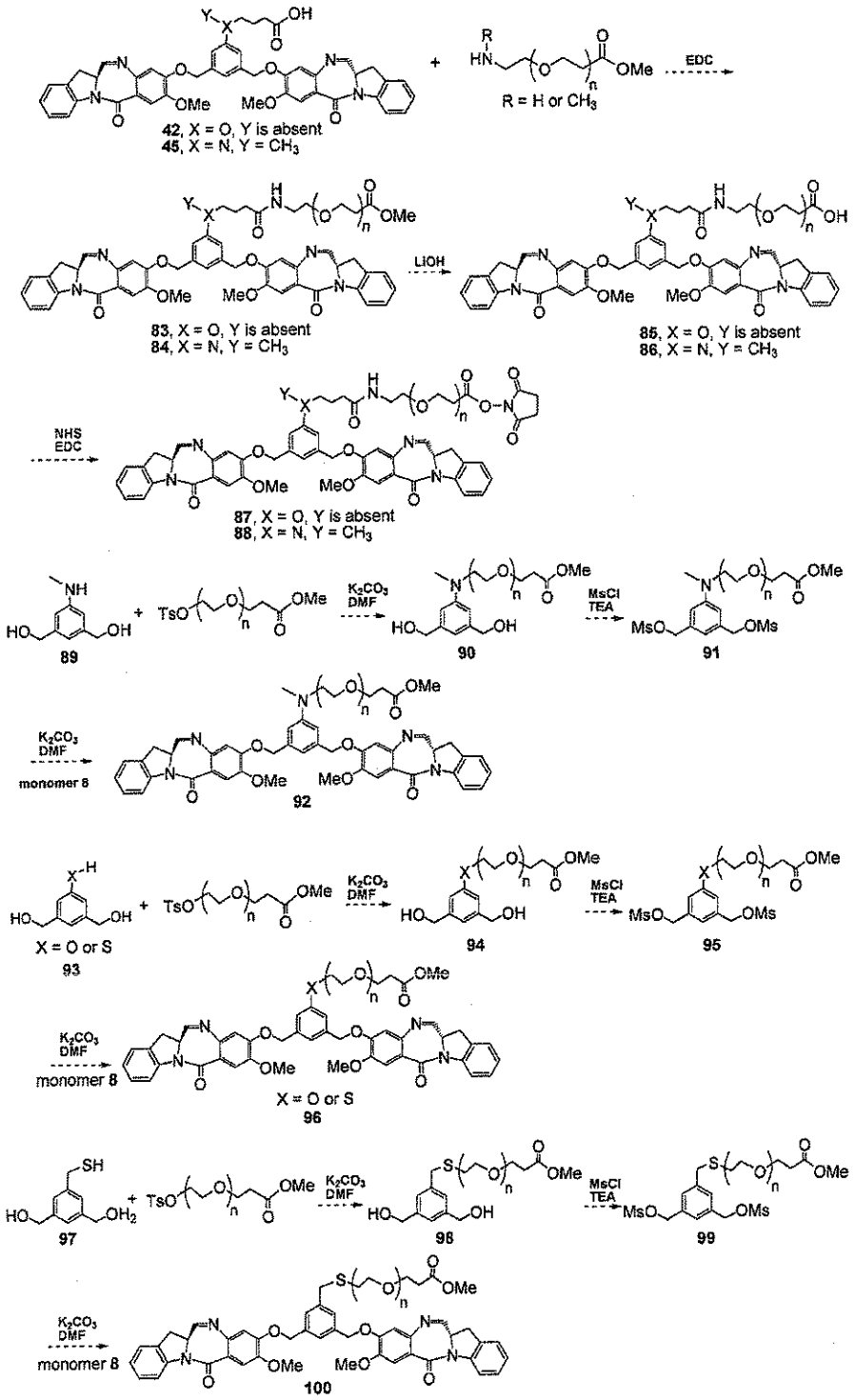


Figure 15. Synthetic schemes of dimers **105** and **110** containing $(PEG)_n$ moiety on the branched linkers

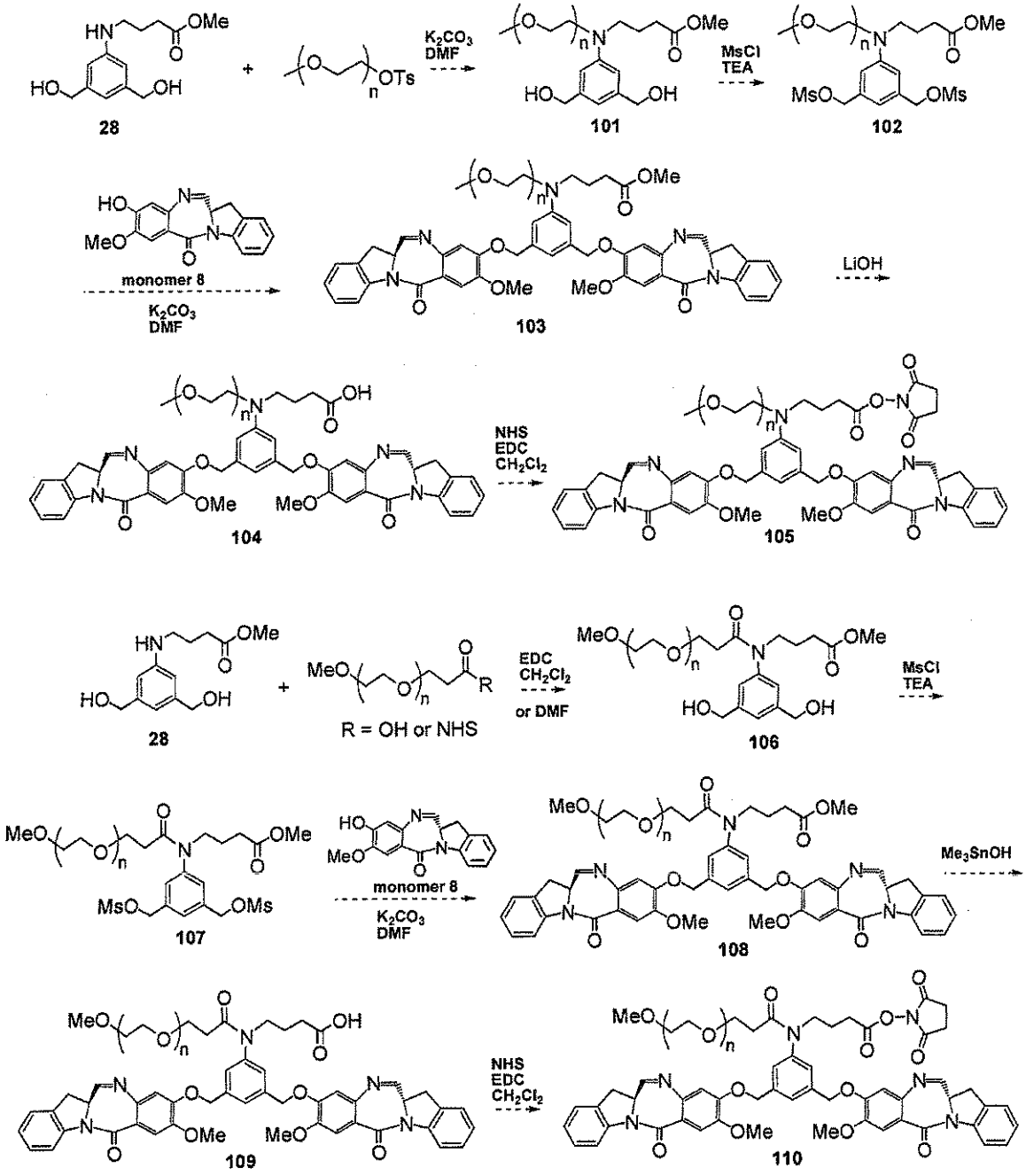


Figure 16. Synthetic schemes of compounds **115**, **119** and **121**

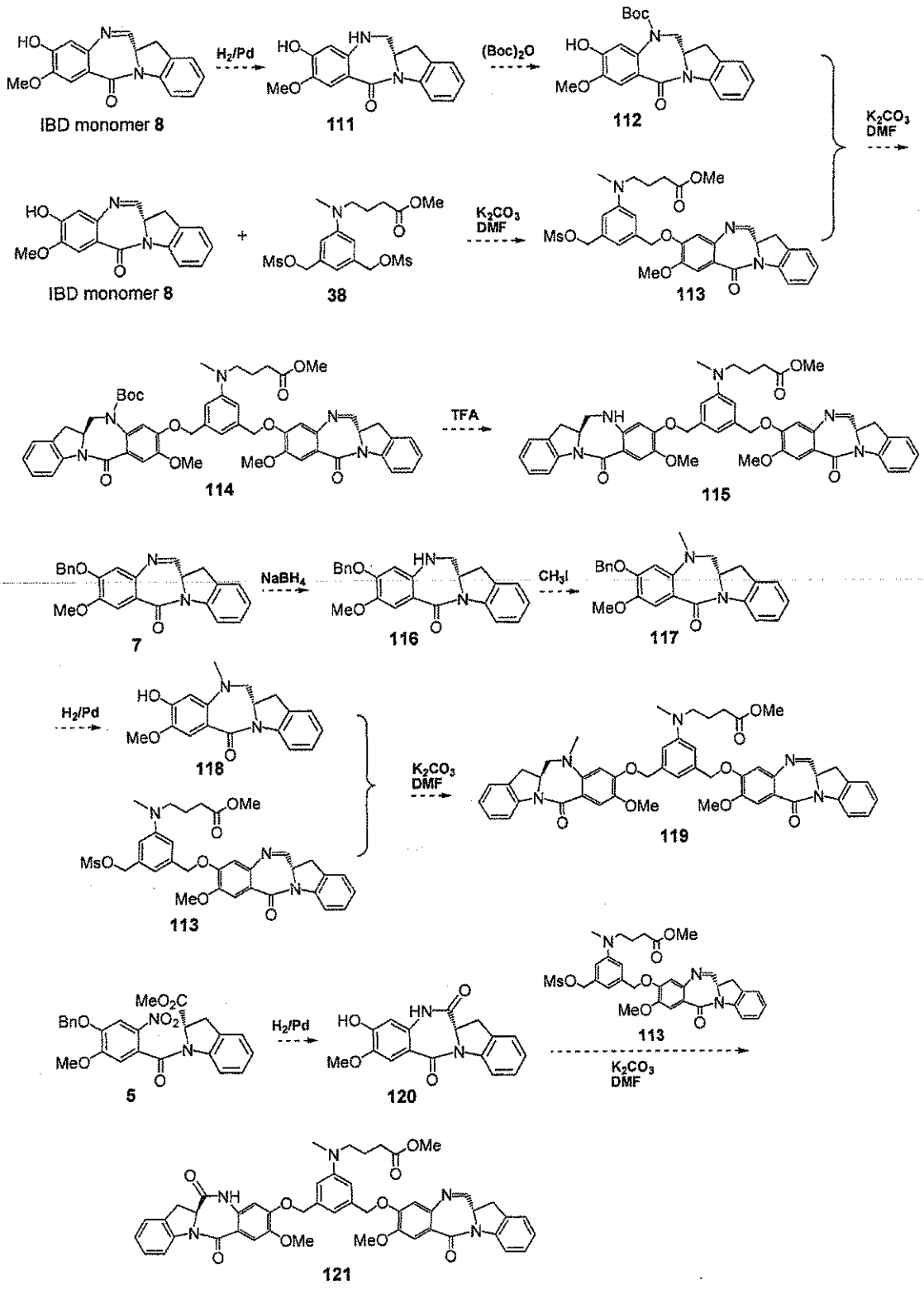


Figure 17. Synthetic scheme of compound **127** (**IGN-11**)

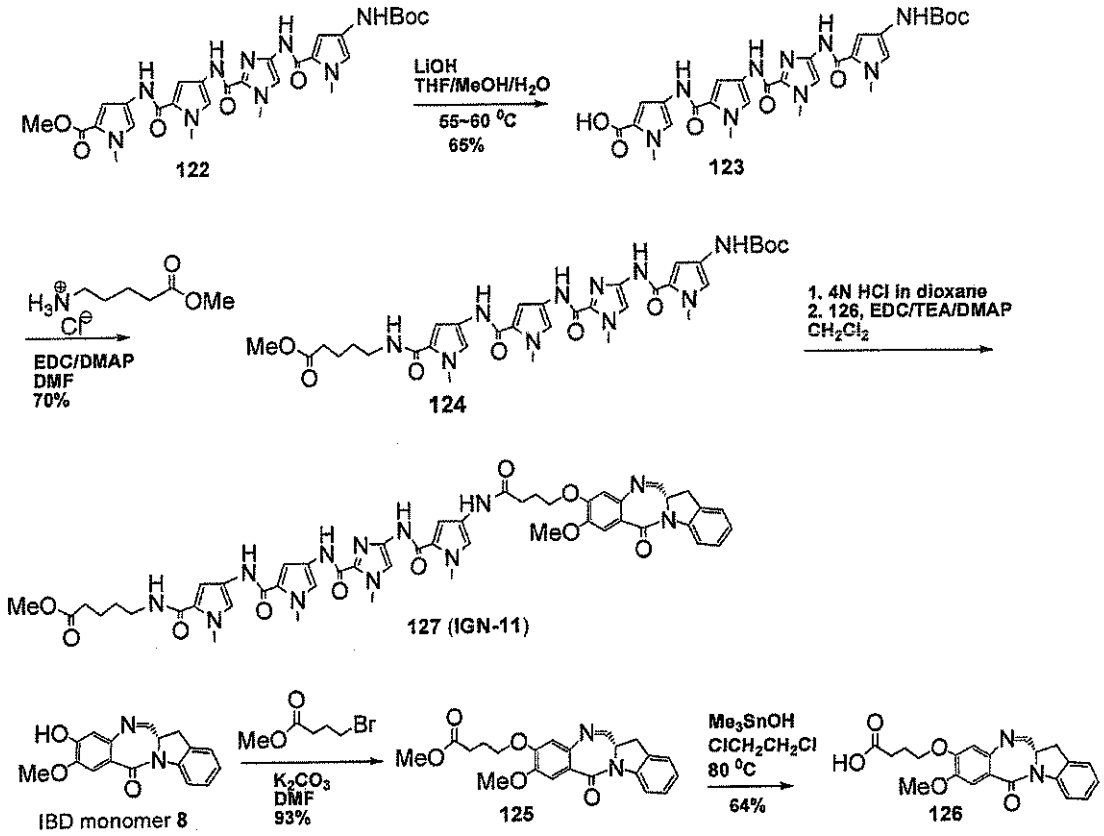


Figure 18. The assembling of polypyrroles/polyimidazoles

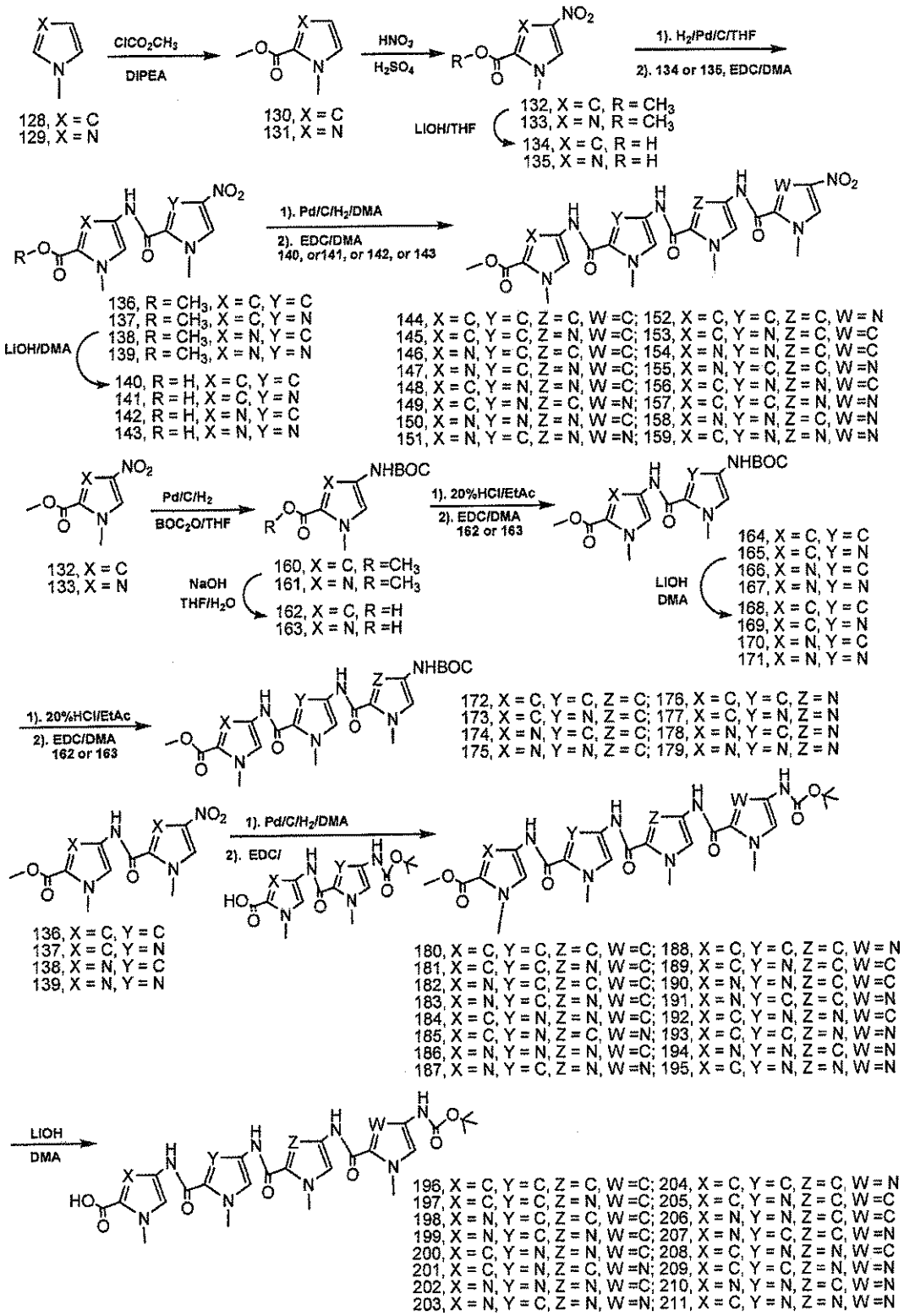


Figure 19. The synthesis of IBD-polypyrrole-imidazole analogs

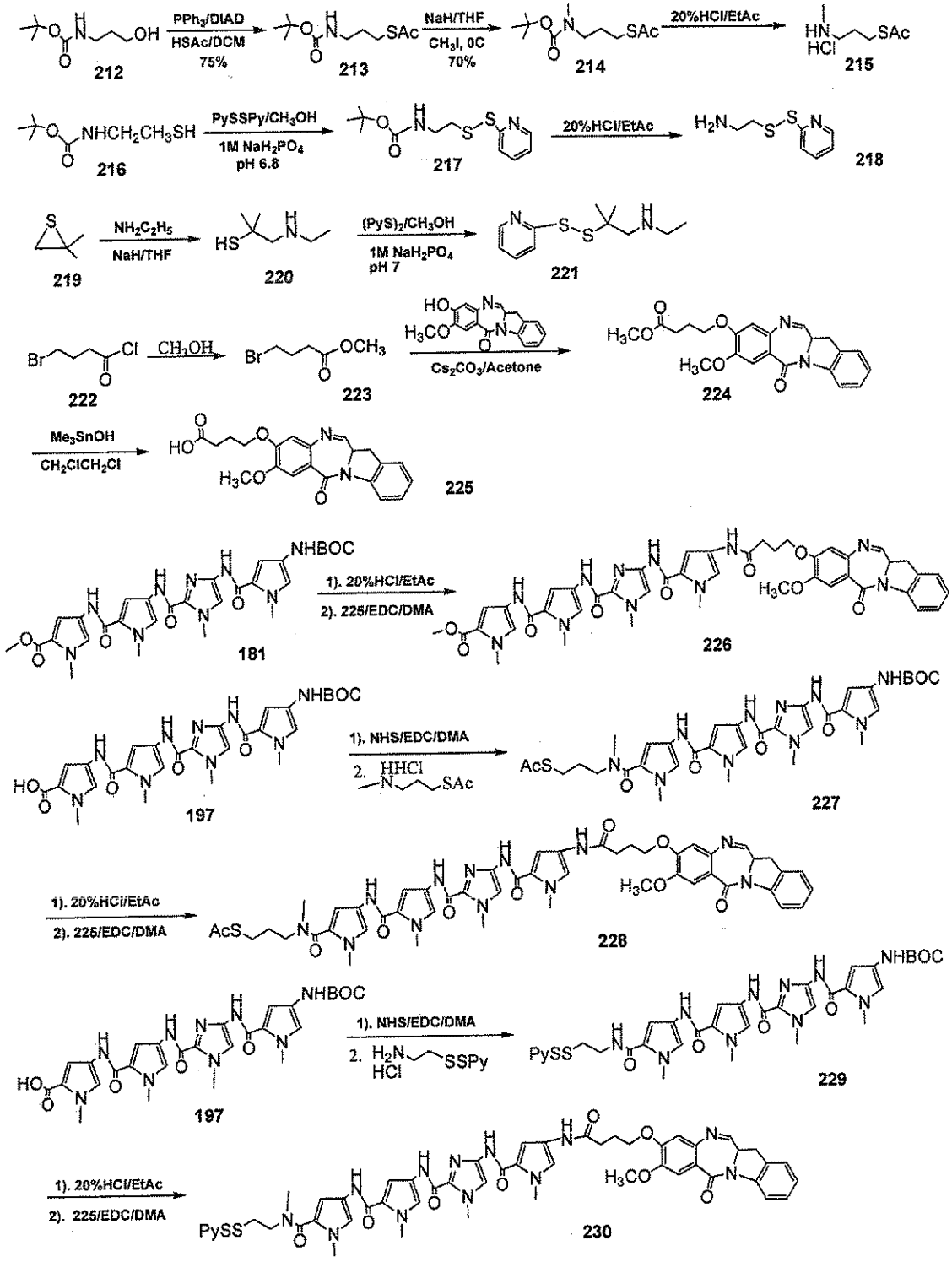


Figure 20. The synthesis of piperidinobenzodiazepine conjugated to antibody through a hydrazone linkage

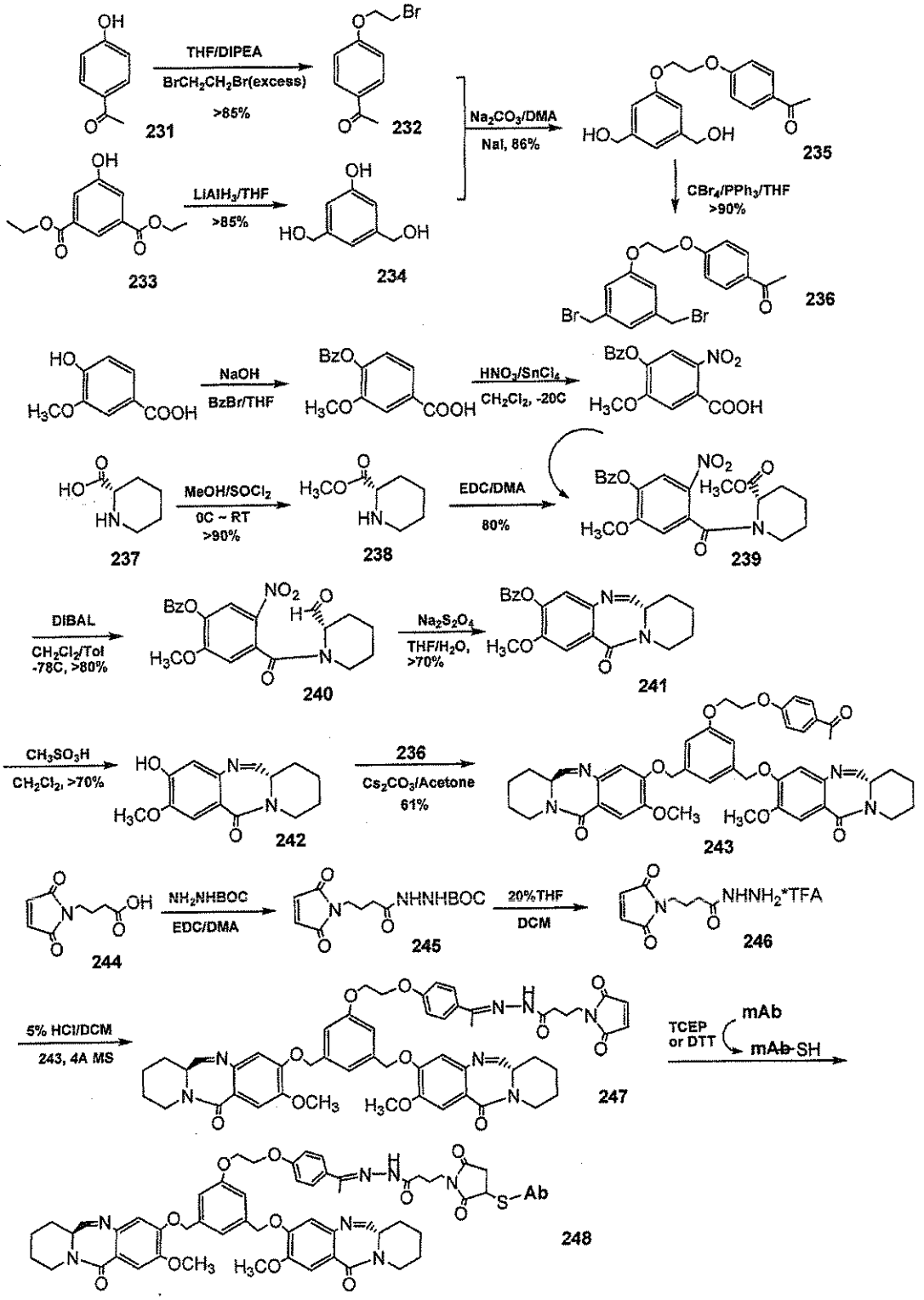


Figure 21. Antiproliferative activity of muB38.1-IGN-03 against COLO205 (Ag+), COLO205 MDR (Ag+), and Namalwa cells (Ag-).

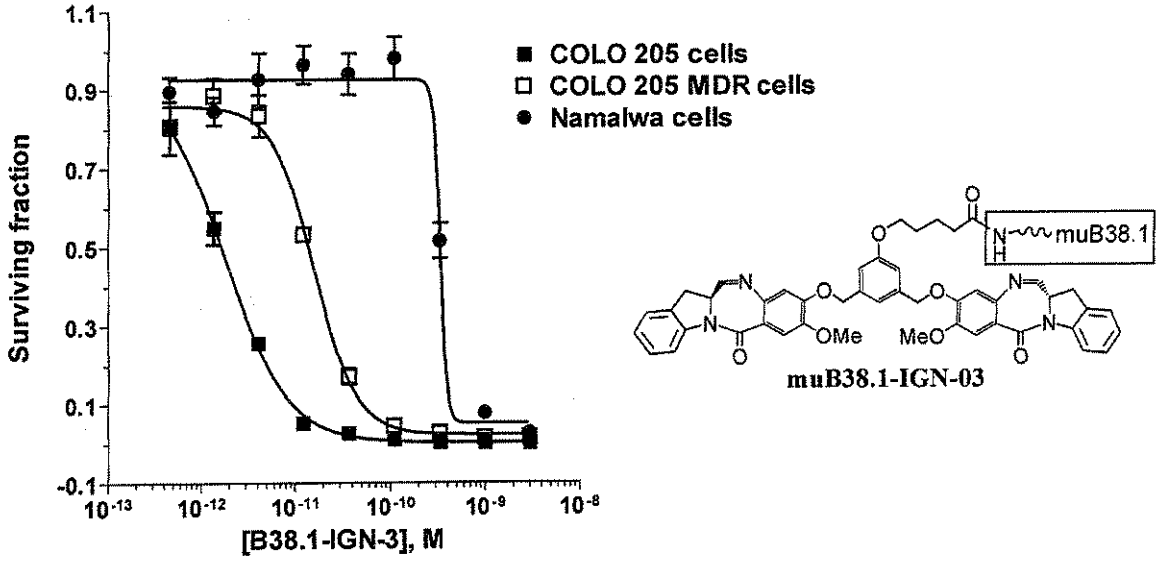


Figure 22. Antiproliferative activity of huN901-IGN-03 against RH-30 (Ag+) cells with and without blocking of antigen binding sites using 1μM huN901.

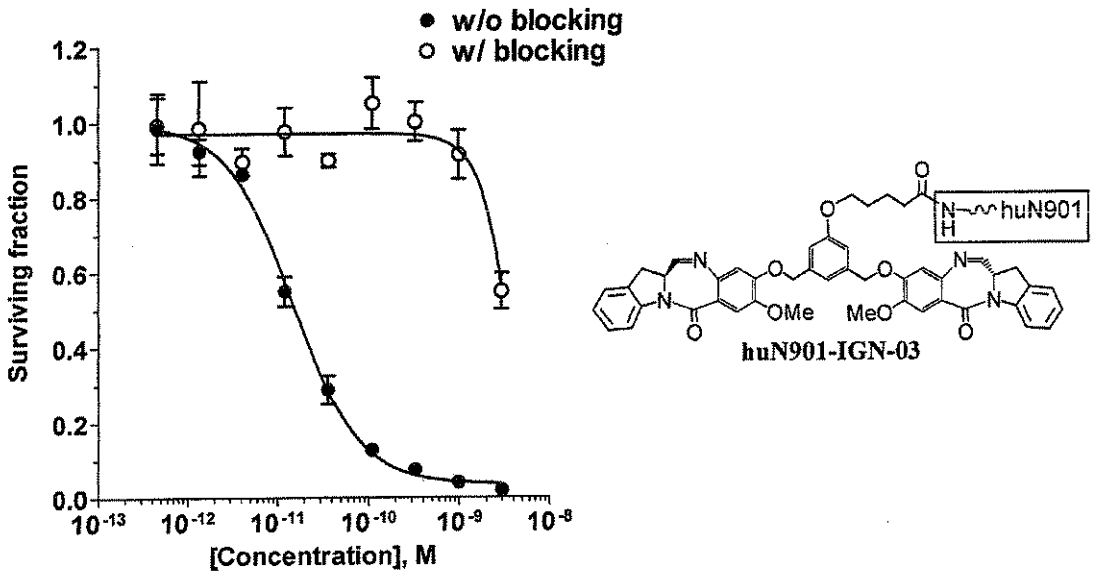


Figure 23. Antiproliferative activity of huN901-IGN-07 against RH-30 (Ag+) cells. Conjugates were tested at three different ratios of cytotoxic agent per antibody (D/A).

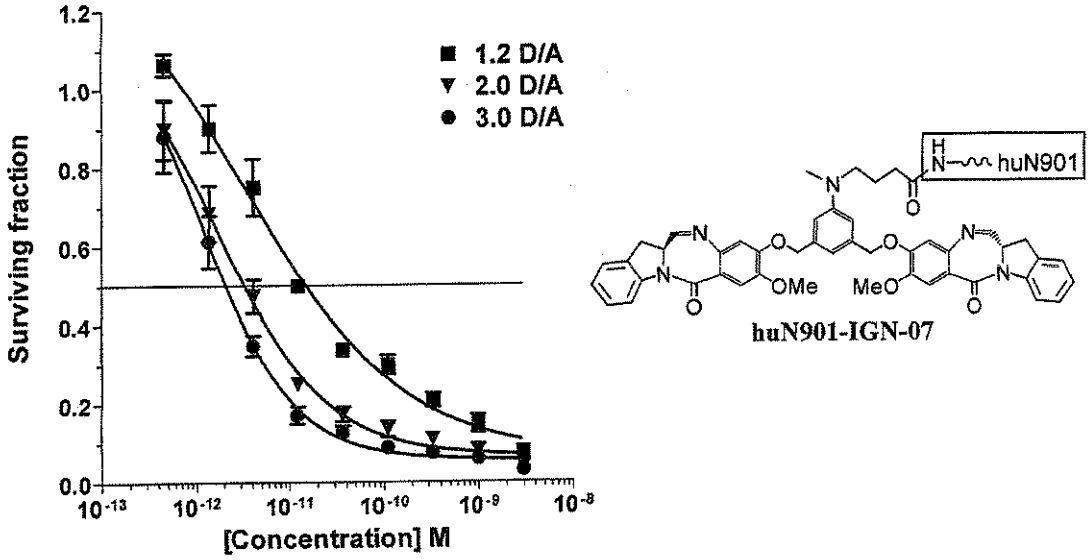


Figure 24. Antiproliferative activity of huN901-IGN-07 (1.2-3.0 D/A) and huN901-IGN-03 (1.7 D/A) against Molp-8 (Ag+) cells.

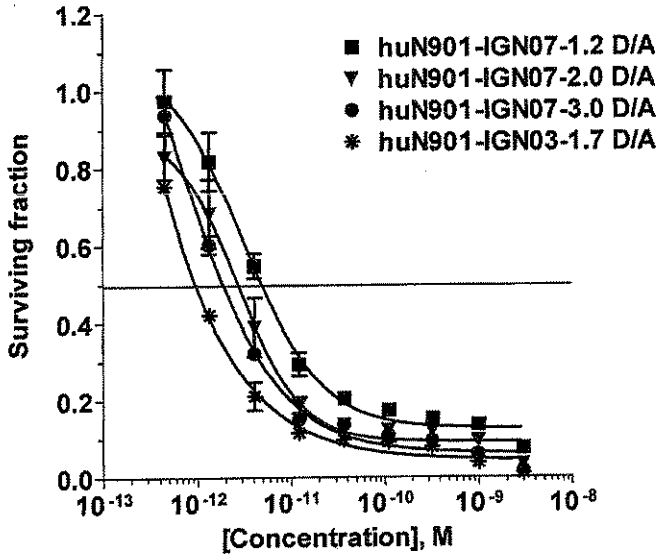


Figure 25. Antiproliferative activity of huN901-IGN-07 (1.2-3.0 D/A) and huN901-IGN-03 (1.7 D/A) against Namalwa (Ag-) cells.

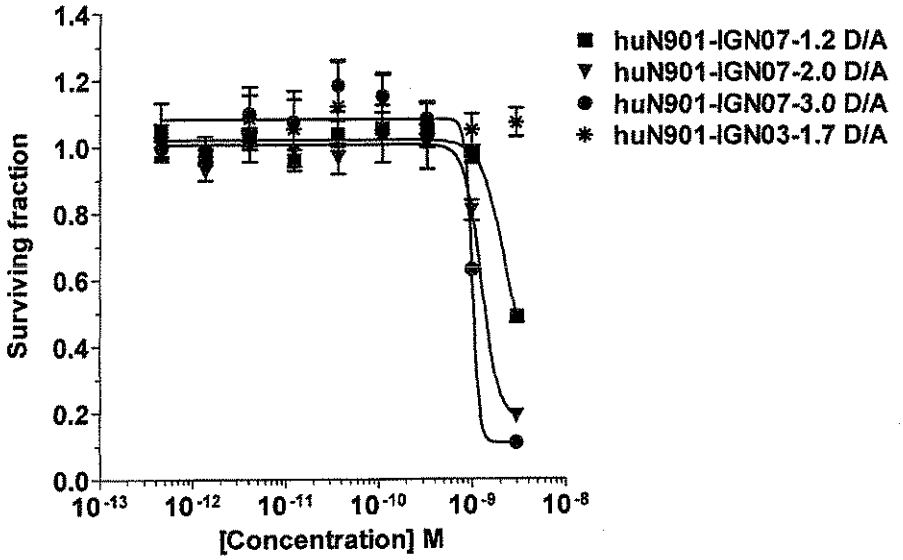


Figure 26. Antiproliferative activity of muB38.1-IGN-10 against COLO 205 (Ag+) and Ramos (Ag-) cells.

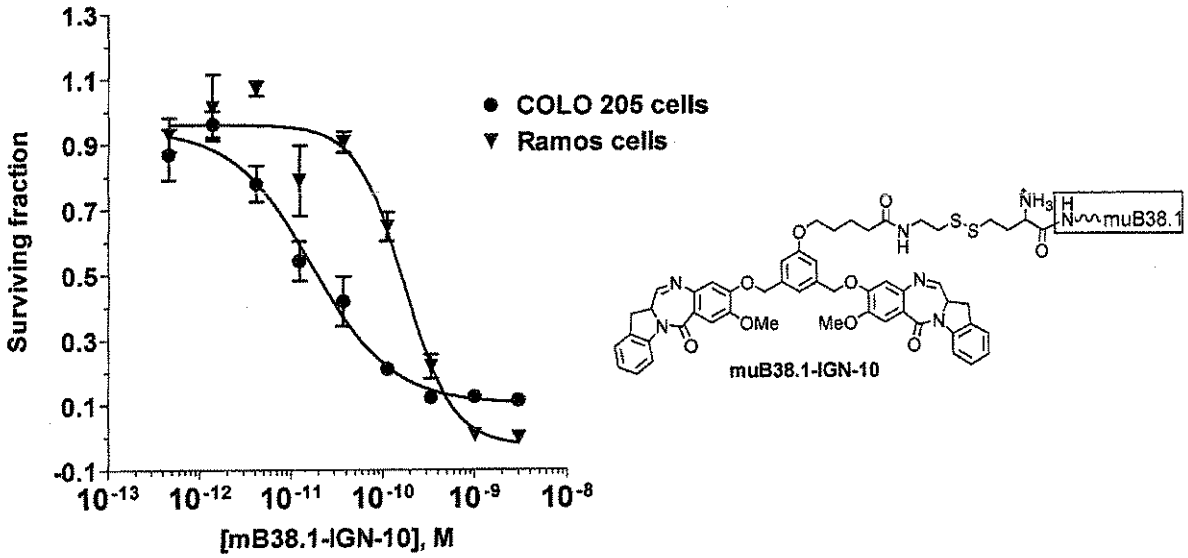


Figure 27. Tumor regression data for single iv dosing of huN901-IGN-07 in nude mice bearing Molp-8 tumors.

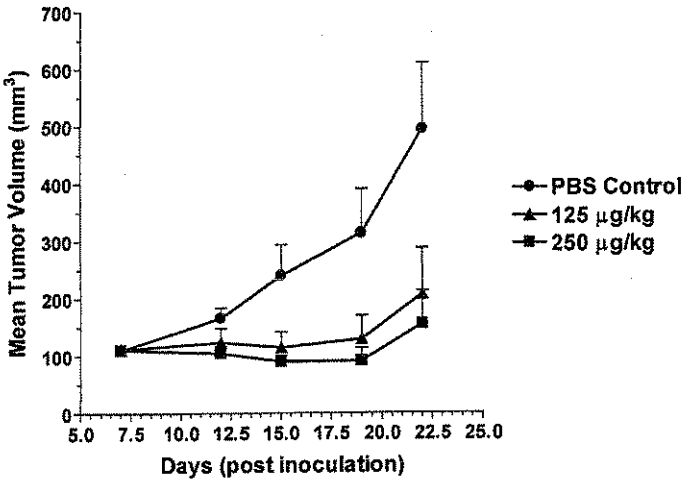


Figure 28. A) Reverse phase ion pair chromatography showing time dependent formation of a covalent adduct between IGN-1 and a 12 base pair duplex DNA probe containing guanines on opposite strands. B) UV-Vis spectra of DNA probe and IGN-1-DNA adduct.

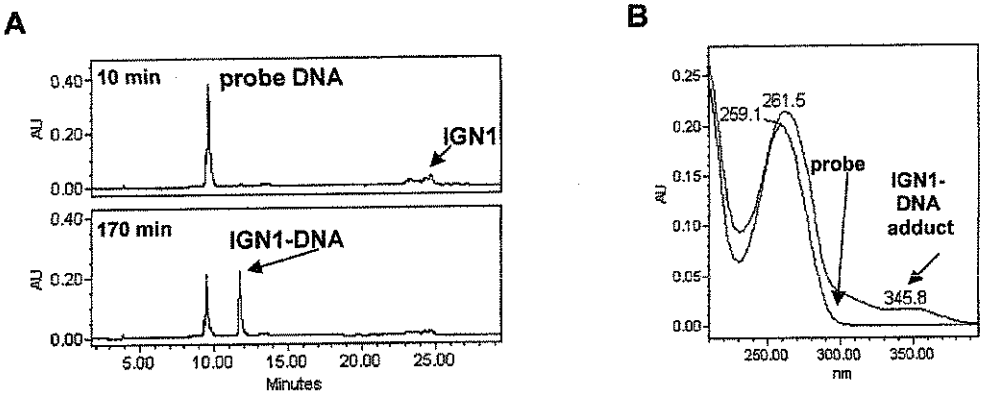


Figure 29. Initial rate of IGN1-DNA adduct formation is dependent on DNA sequence. IGN1 binds faster to DNA containing an internal GATC motif than DNA with a GTAC sequence. DNA probe substituted with deoxyInosine (I) (containing no C-2 amino group) in place of guanine (G) showed no reaction with IGN-1.

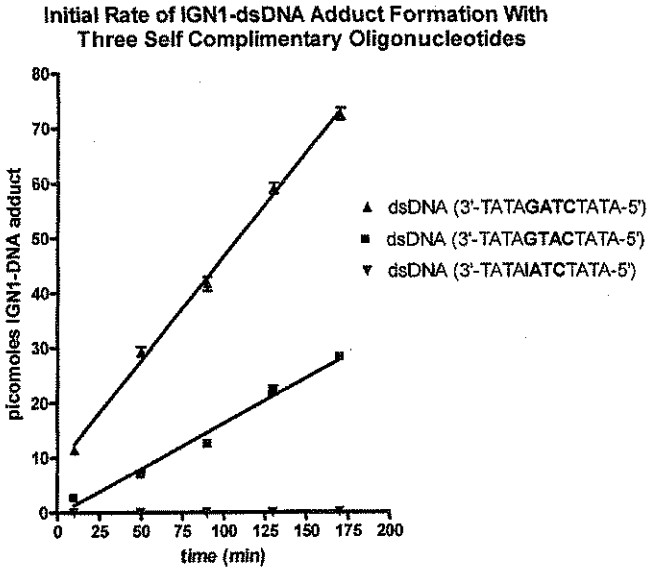


Figure 30. IGN-01, IGN-02 and IGN-09 tested for binding and crosslinking to double stranded self-complimentary probe DNA.

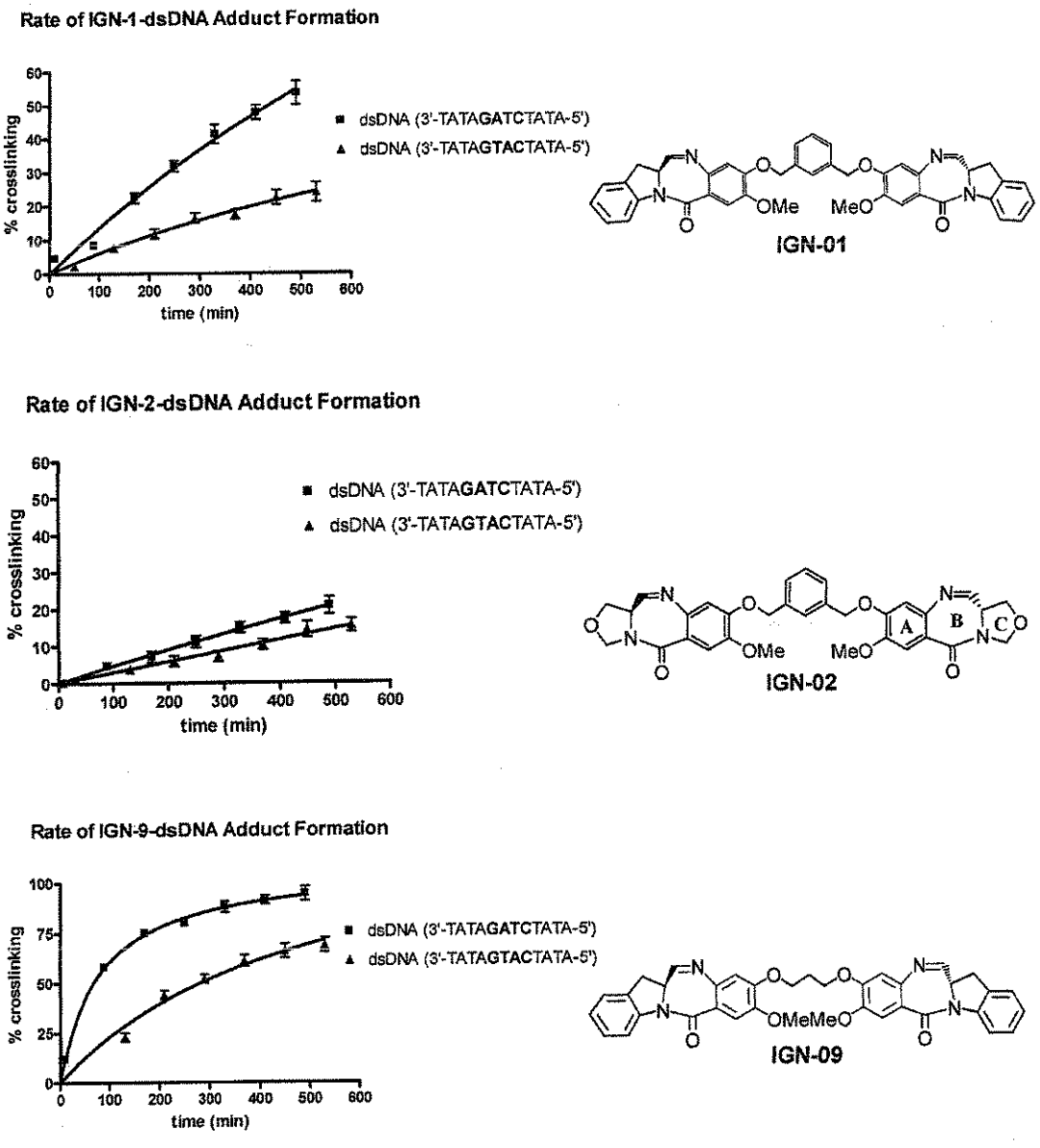


Figure 31

Table 1. Indolinobenzodiazepine dimers and oxazoloidinobenzodiazepine dimer antiproliferative activity on a variety of cancer cell lines. IC50 values (pM) are shown for each compound tested in a 5 day continuous exposure assay.

	IC50s (pM)										
Dimers	HL60/ATCC	Ramos	MDA-MB-231	SK-MEL-28	BJAB	Molt-4	RH-30	COLO 205	COLO 205-MDR	Namalwa	Namalwa-MDR
IGN-01	<0.46	<0.46	1.4	44							
IGN-02	450	67	1400	4700							
IGN-03	3.2	0.64	16	14							
IGN-04					1.9	2.7					
IGN-05		0.65			1.0		3.9				
IGN-06		1.5					3.7			4.2	
IGN-07		1.9					5.9			4.7	
IGN-08		5.8					22			7.0	
IGN-09		<0.46					7.8	14	61	1.4	13

Figure 32

Table 2. Comparison of the IC50s for the dimers with and without linkers

Dimers	IC50s (pM)
	Ramos cells
IGN-01	<0.46
IGN-09	<0.46
IGN-03	0.64
IGN-05	0.65

Figure 33. Synthetic scheme for indolinobenzodiazepine (IBD) dimers

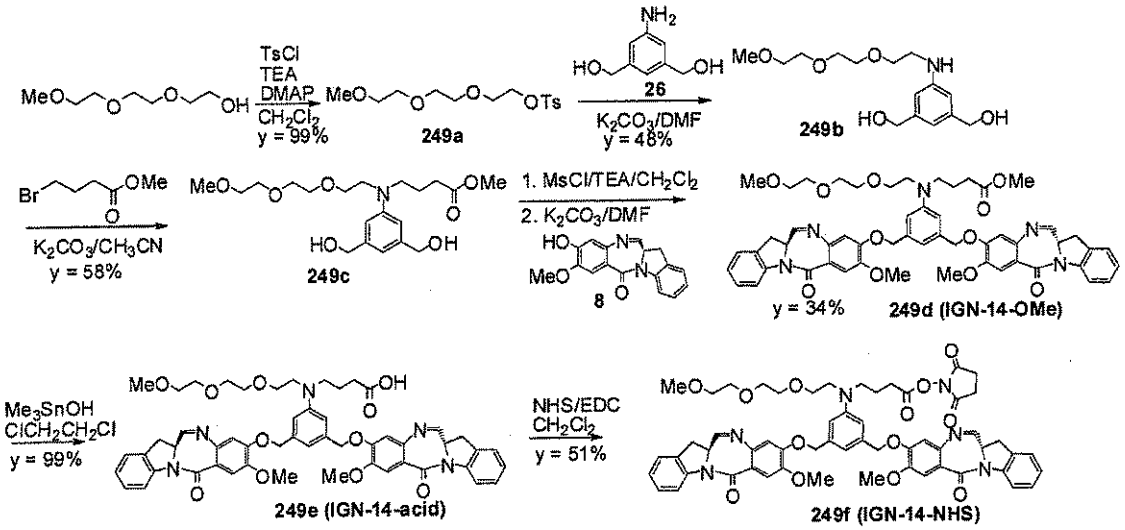


Figure 34. Synthetic scheme of esters of IBD dimers

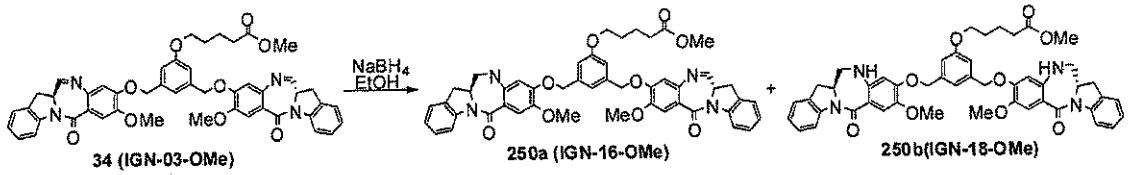


Figure 35. Synthetic scheme of dimer **251b (IGN-17-OMe)**.

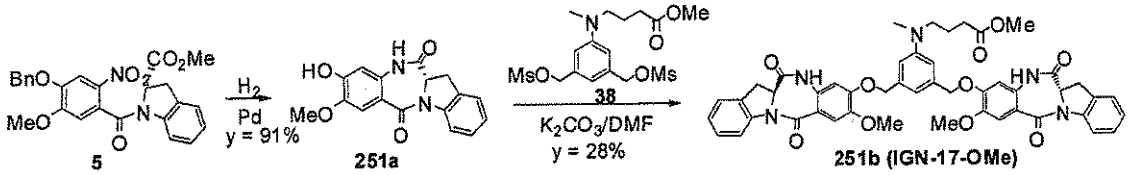


Figure 36. Synthetic scheme for dimer **252b (IGN-19-OMe)**.

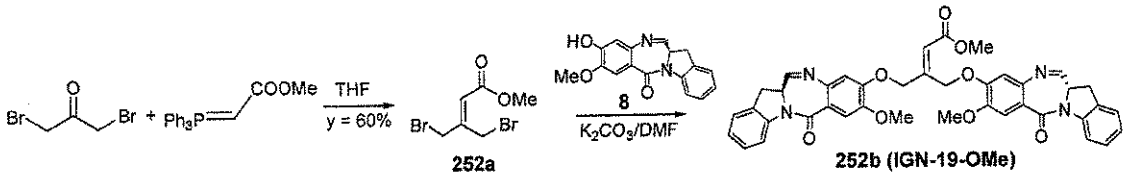


Figure 37. Synthetic scheme for linkable dimer

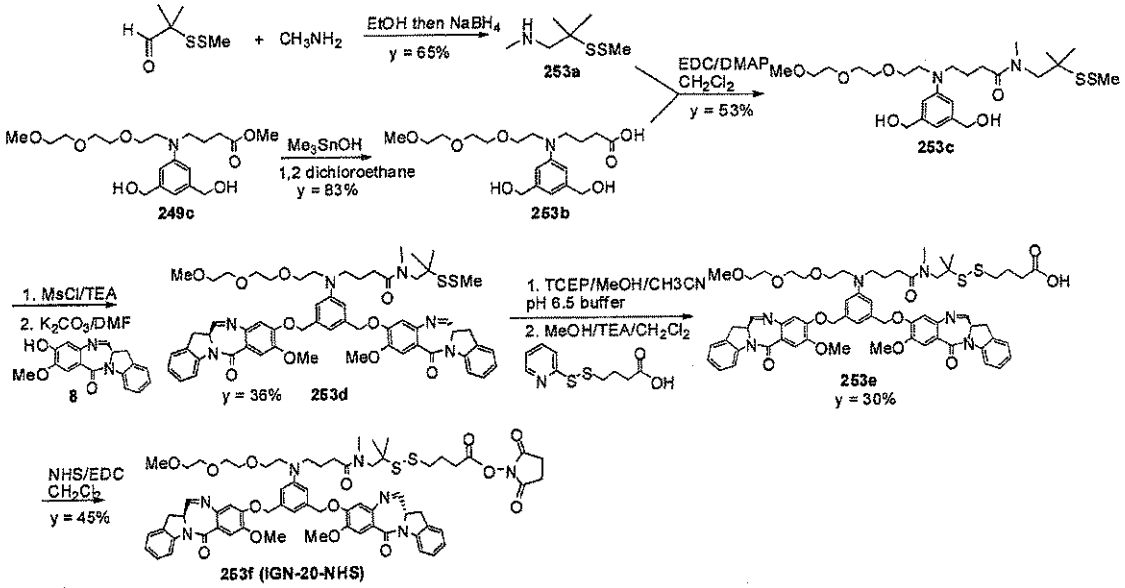


Figure 38. Synthetic scheme of linkable compounds **254d (IGN-23-NHS)** and **254f (IGN-24-NHS)**.

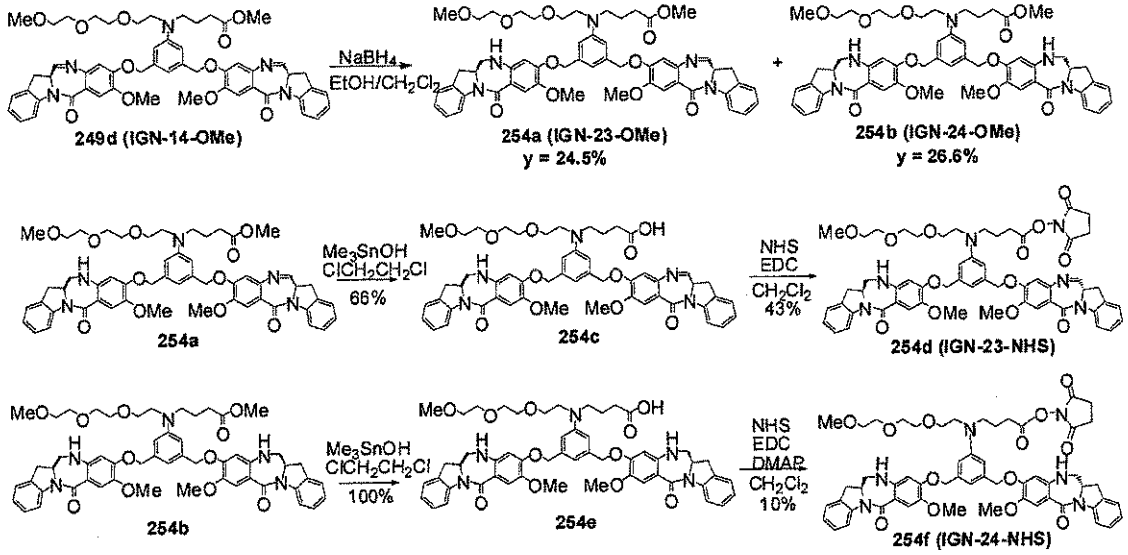


Figure 39. Synthetic scheme of IBD dimer **255c (IGN-26-OMe)**.

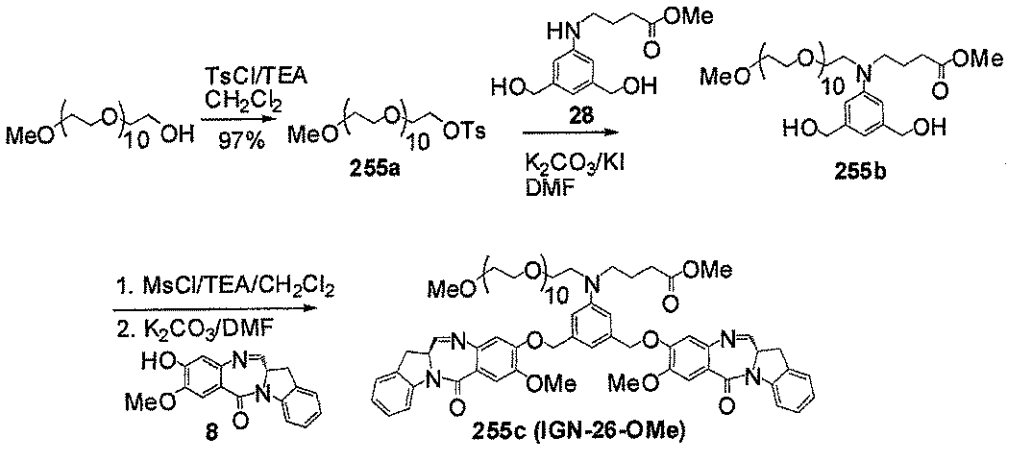


Figure 40. Synthetic scheme of compound **256g (IGN-29-NHS)**.

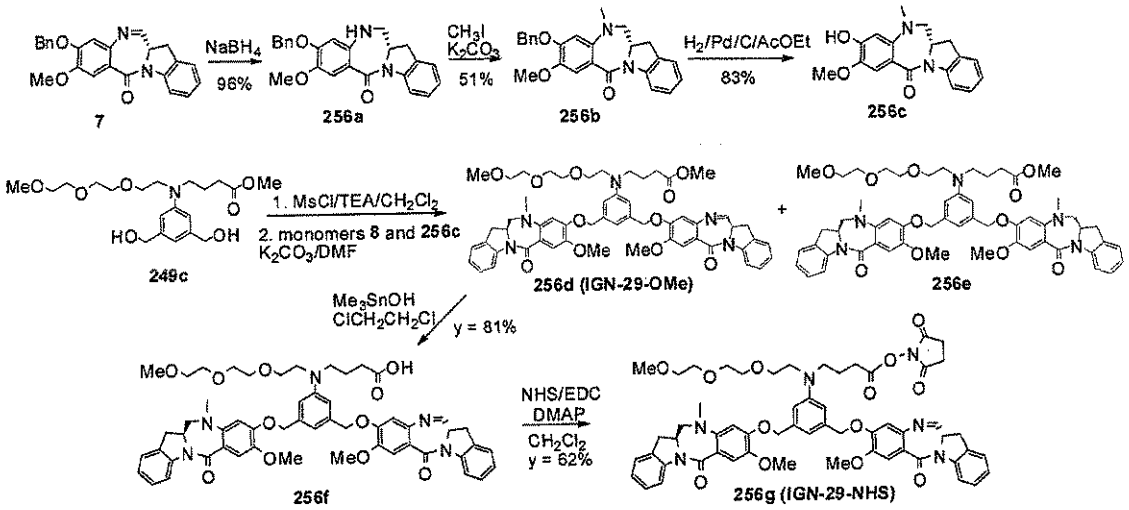


Figure 41. Synthetic scheme of compound **257e (IGN-33-NHS)**.

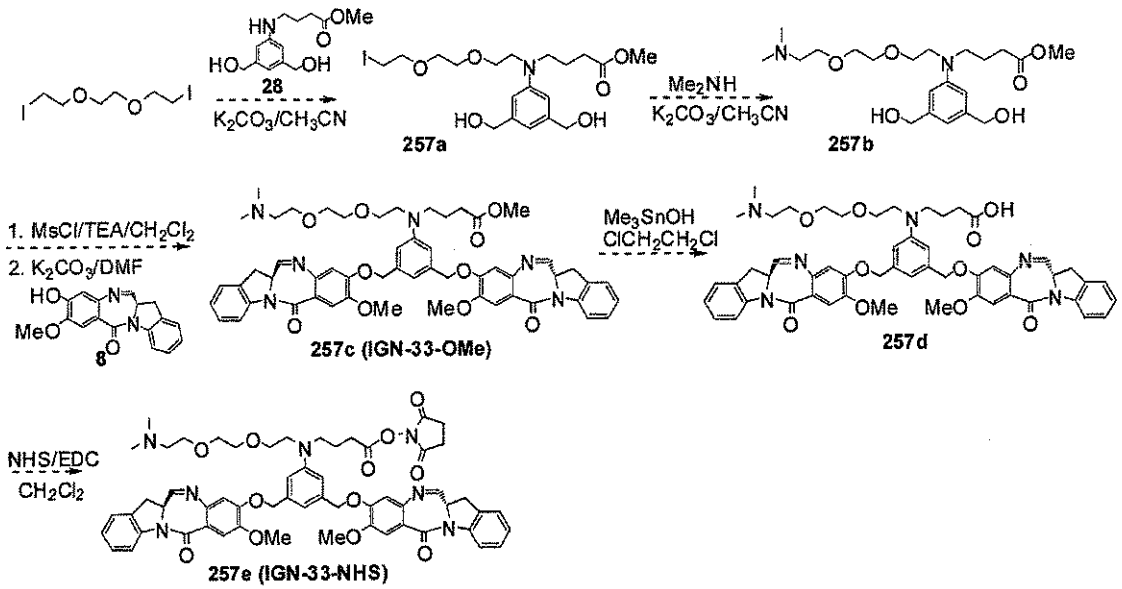


Figure 42. Synthetic scheme of compounds **258h (IGN-15-SMe)** and **259b (IGN-21-SMe)**.

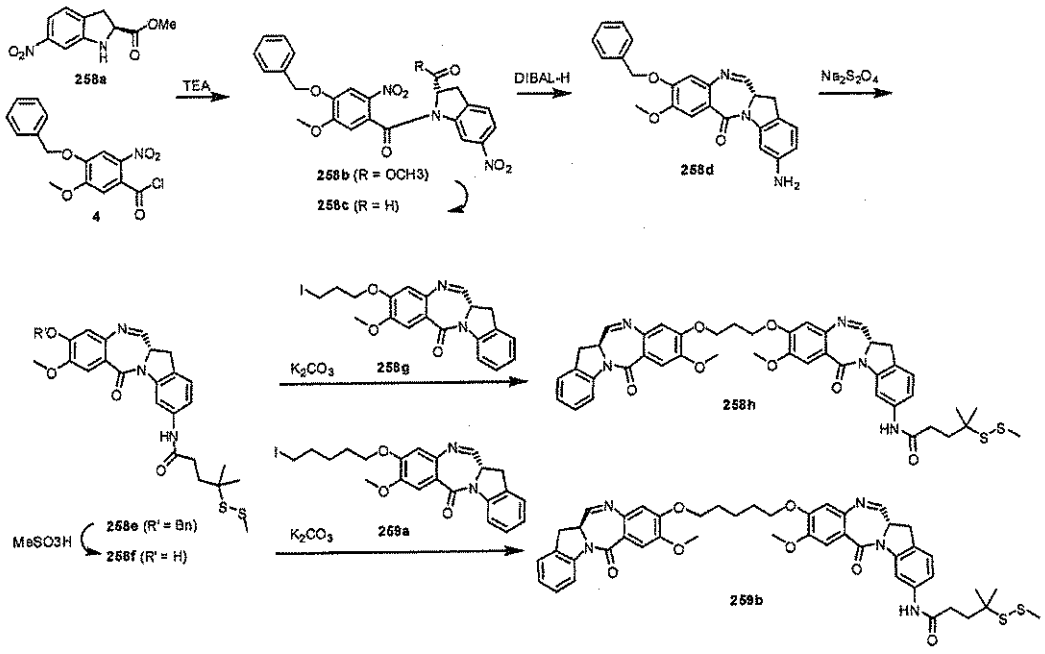


Figure 43. Synthetic scheme of compound **260c (IGN-25-OMe)**.

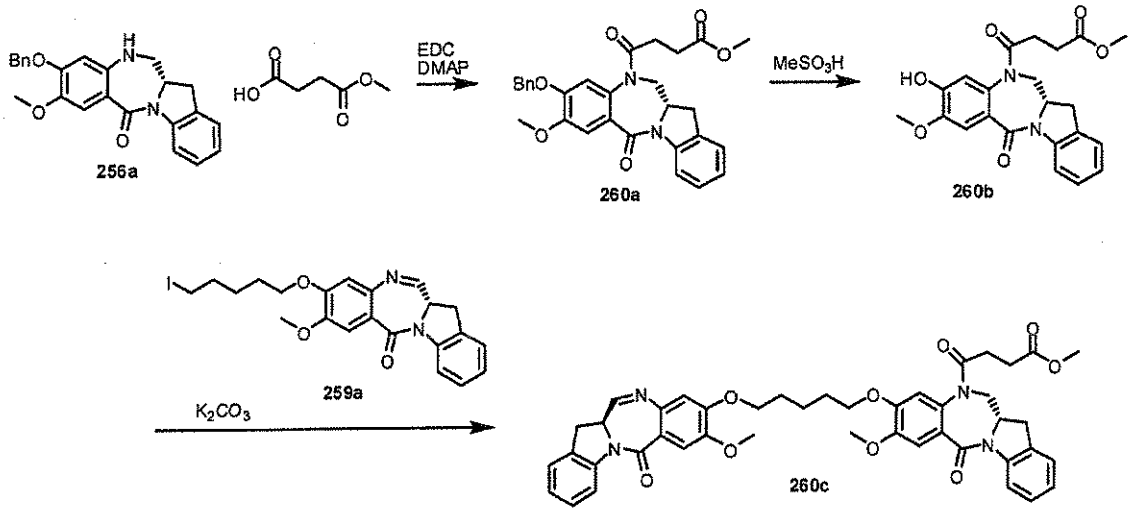


Figure 44. Synthetic scheme of compounds **261e** (TBD monomer) and **262 (IGN-30-OMe)**.

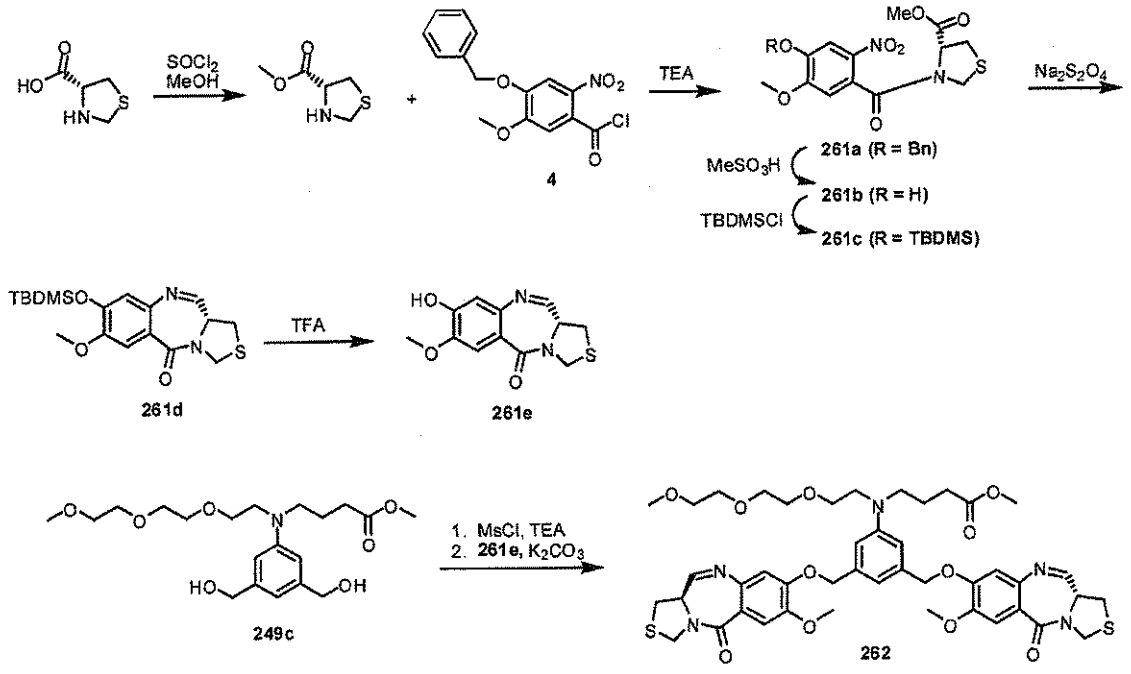


Figure 45. Synthetic scheme of dimer **263e (IGN-13-NHS)**.

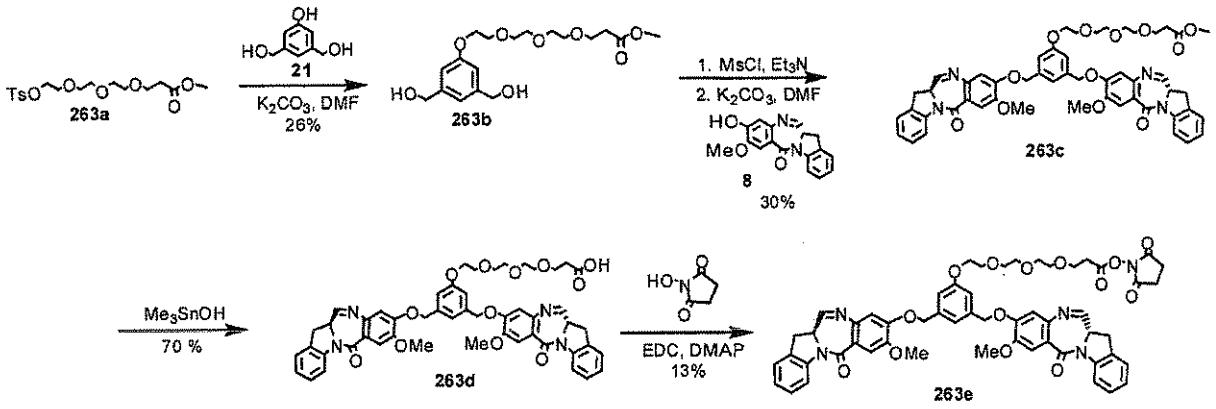


Figure 46. Synthetic scheme of dimer **264e (IGN-27-NHS)**.

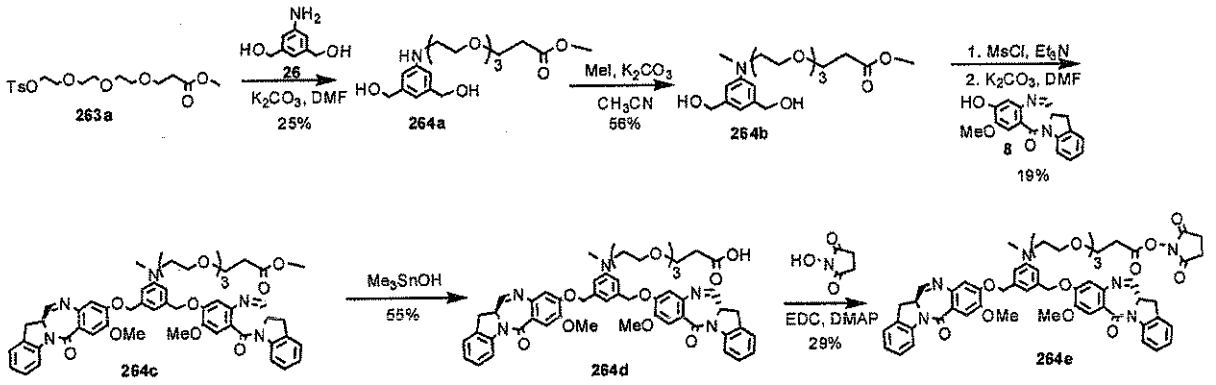


Figure 47. Synthetic scheme of dimer **265g (IGN-28-NHS)**.

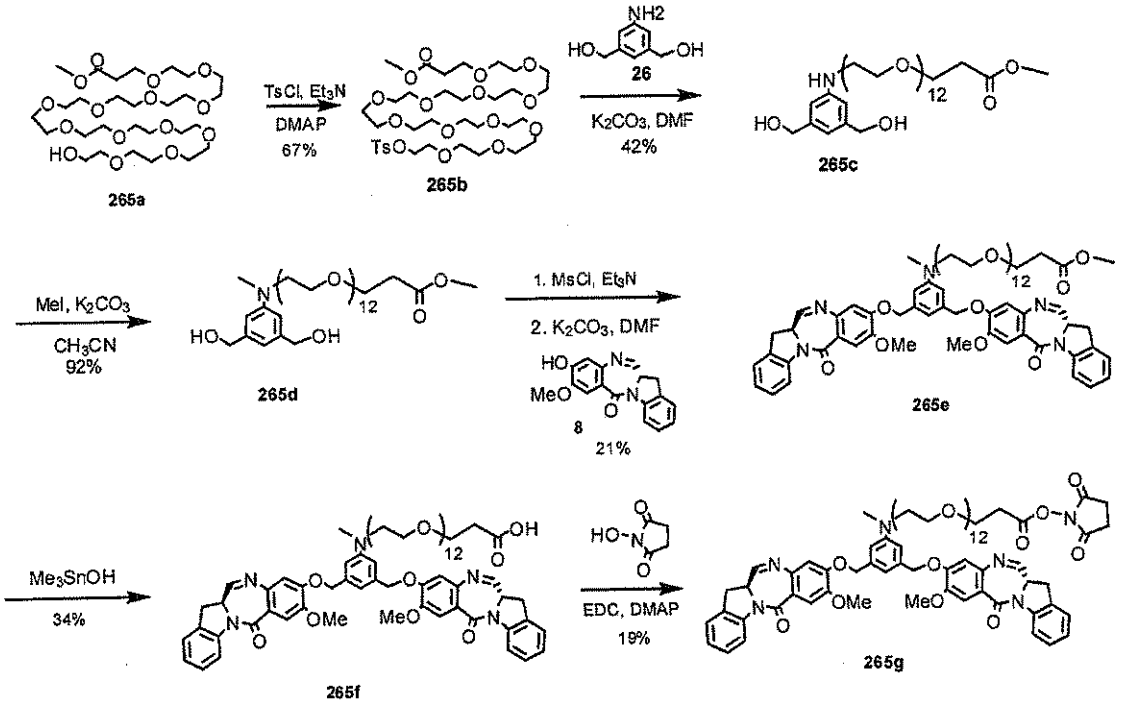


Figure 48. Synthetic scheme of dimer **266c (IGN-22-OMe)**.

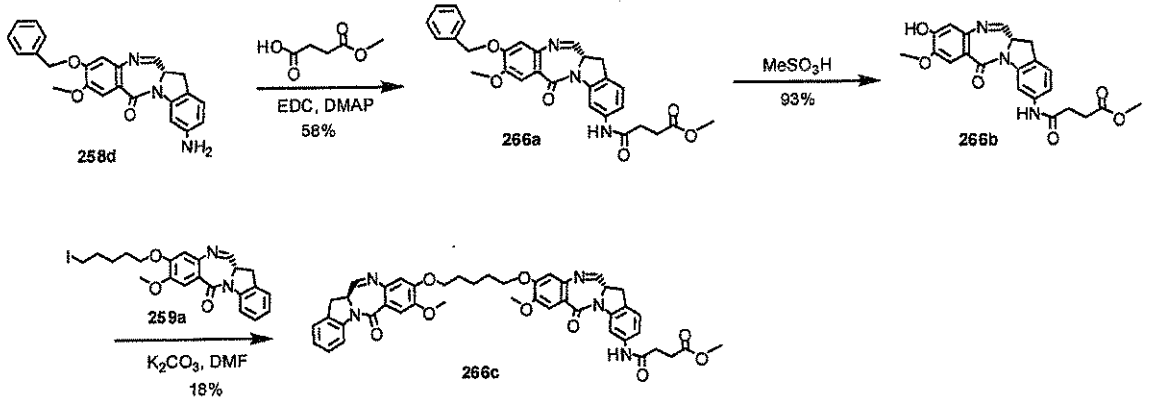


Figure 49. Synthetic scheme of dimer **267d (IGN-31-SMe)**.

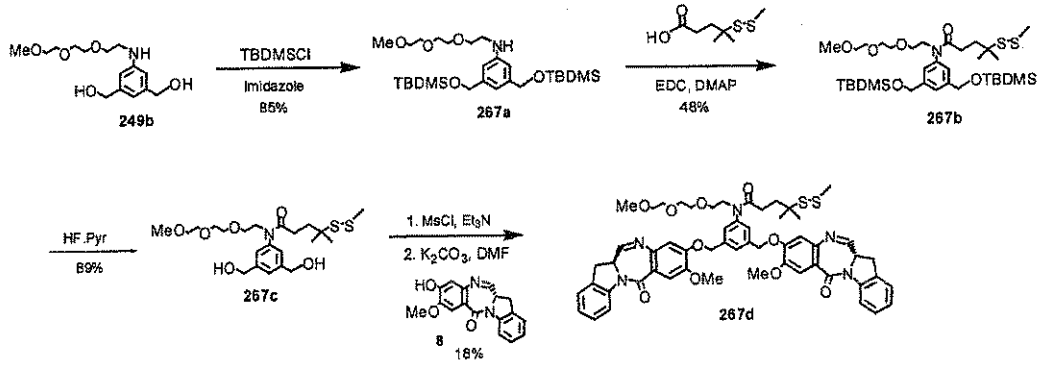


Figure 50. Synthetic scheme of dimer **268b (IGN-32-OtBu)**.

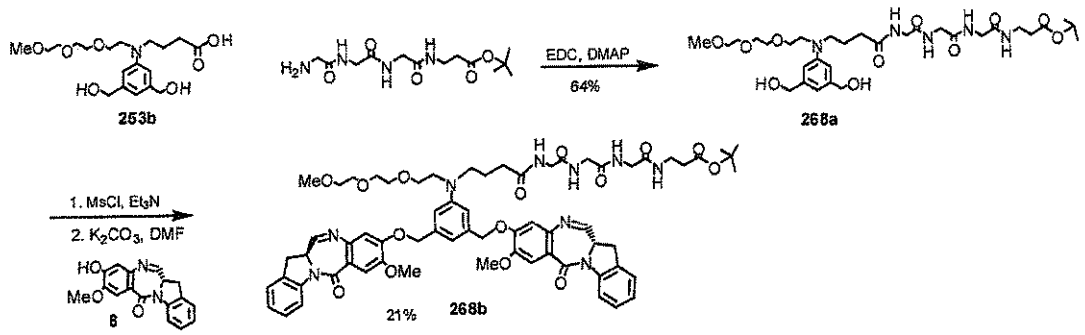
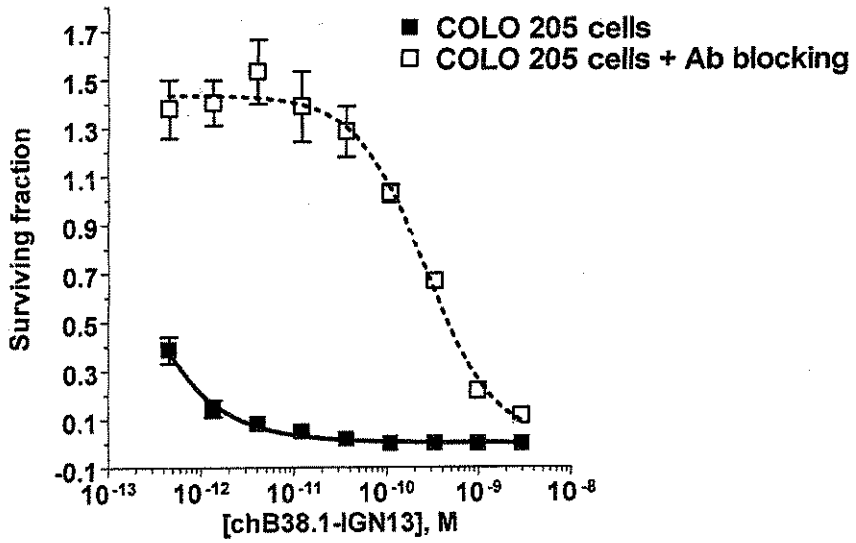


Figure 51. In Vitro Cytotoxicity of IGN Compounds

	IC50 (nM)					
IGN	Ramos	COLO205	RH-30	Namalwa	KB	LoVo
IGN13-OMe	0.003	0.031	0.009	0.005	0.005	
IGN14-OMe	0.005	0.079	0.025	0.017	0.020	
IGN15-SMe	0.048	3.000	0.520	0.410		
IGN16-OMe	0.003				0.009	0.012
IGN17-OMe	3.000	3.000	0.048	3.000		
IGN18-OMe	0.037				0.890	0.570
IGN19-OMe	0.047				0.350	0.800
IGN20-SMe					1.160	
IGN21-SMe					0.146	
IGN23-OMe					0.138	
IGN24-OMe					0.789	
IGN25-OMe						
IGN26-OMe		3.800		0.200		
IGN27-OMe		0.210		0.015		
IGN28-OMe		1.000		0.130		
IGN30-OMe		2.900		0.320	1.500	

Figure 52. Antiproliferative activity of chB38.1-IGN13 against (A) COLO 205 (Ag+) cells with and without blocking of antigen binding sites and (B) against LOVO (Ag+) cells.

A)



B)

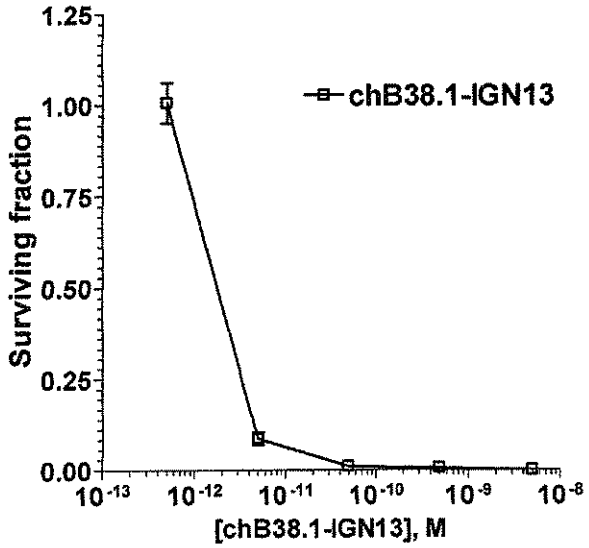


Figure 53. Antiproliferative activity of huMy9-6-IGN13 against NB-4 (Ag+) cells with and without blocking of antigen binding sites.

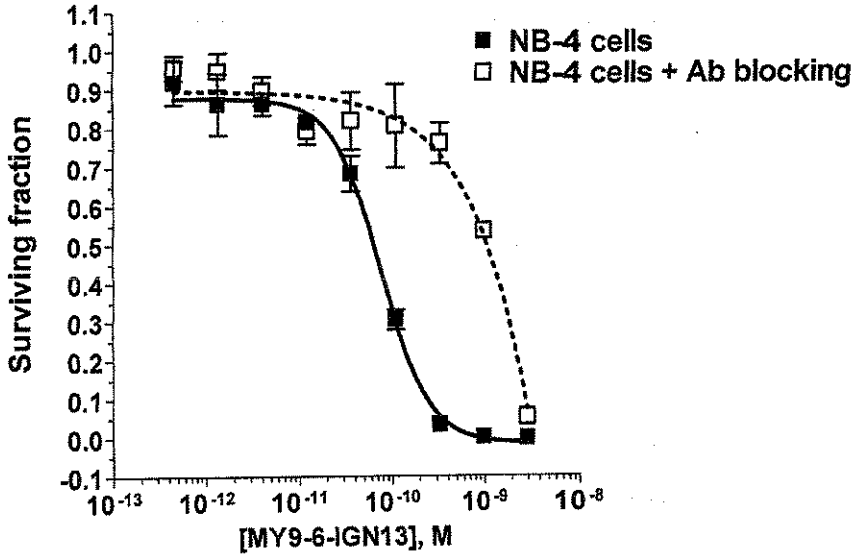
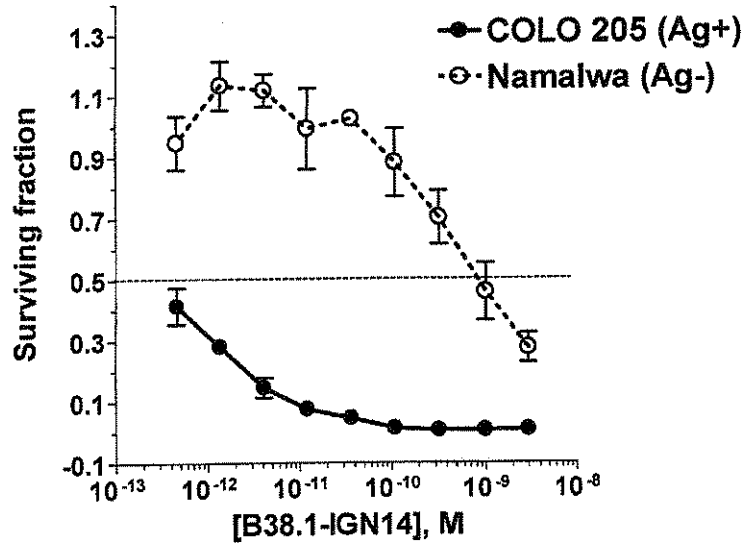


Figure 54. Antiproliferative activity of chB38.1-IGN14 against (A) COLO205 (Ag+) cells and (B) LOVO (Ag+) cells and Namalwa (Ag-) cells

A)



B)

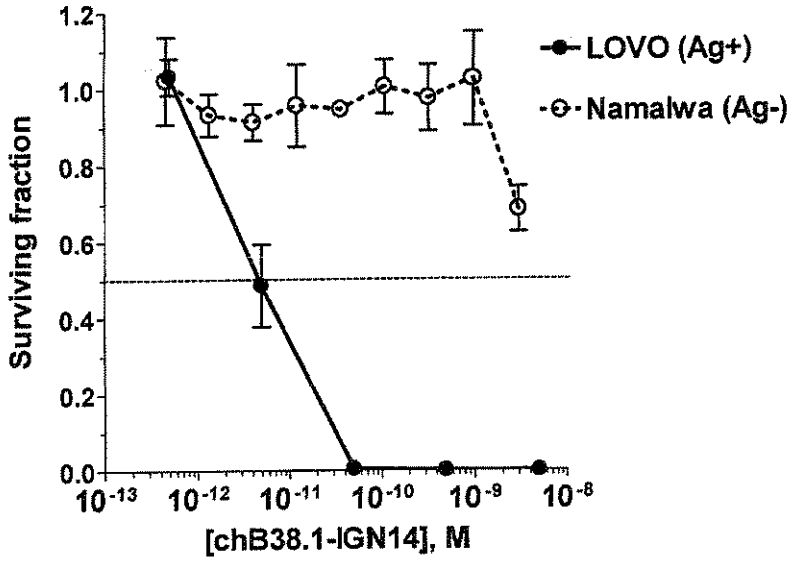


Figure 55. Antiproliferative activity of huMY9-6-IGN14 against NB-4 (Ag+) cells using Namalwa (Ag-) cells as a control.

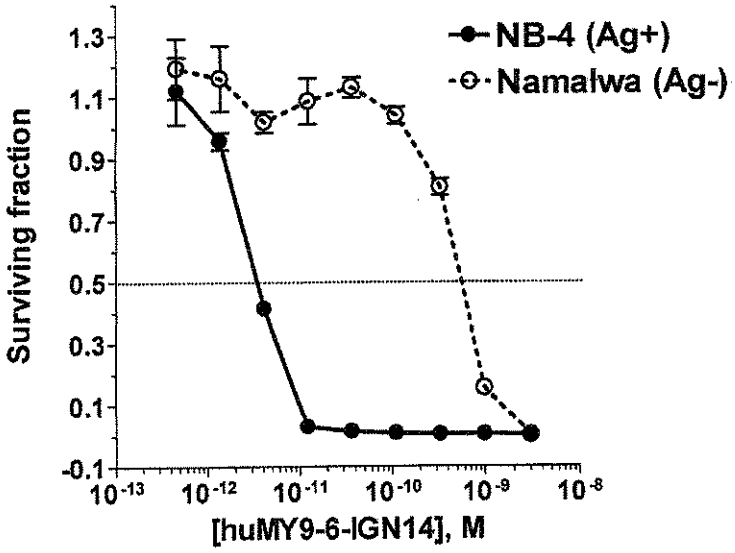
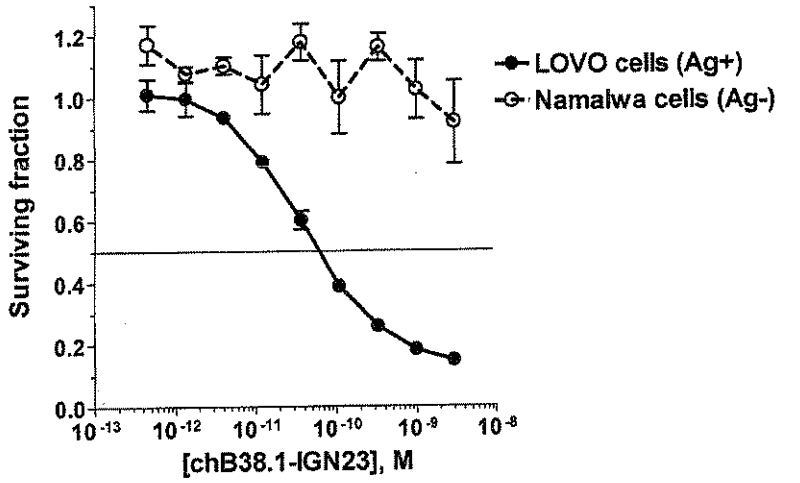


Figure 56. Antiproliferative activity of chB38.1-IGN23 (A) against LOVO (Ag+) cells using Namalwa (Ag-) cells as a control; and (B) against COLO205 (Ag+) cells with and without blocking antigen binding sites.

A)



B)

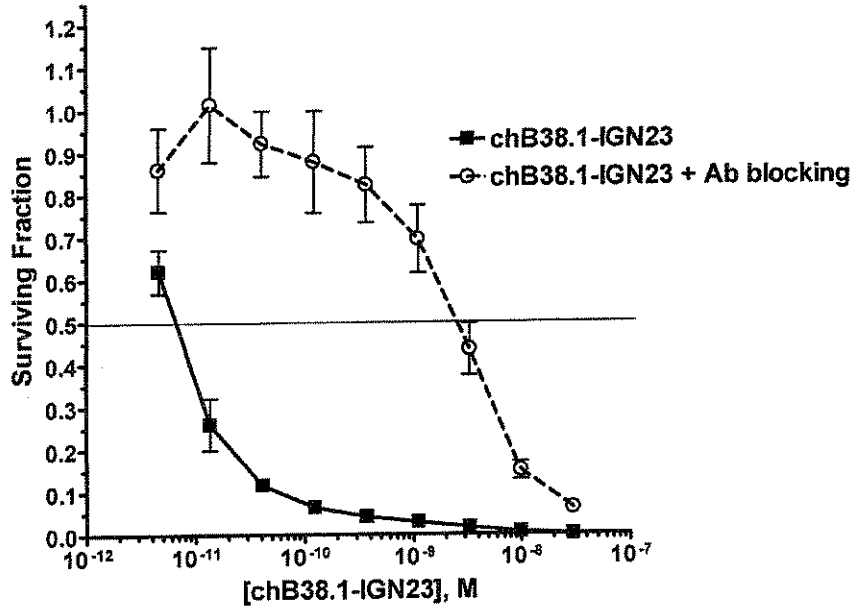


Figure 57. Antiproliferative activity of chB38.1-IGN29 against COLO205 (Ag+) cells with and without blocking antigen binding sites.

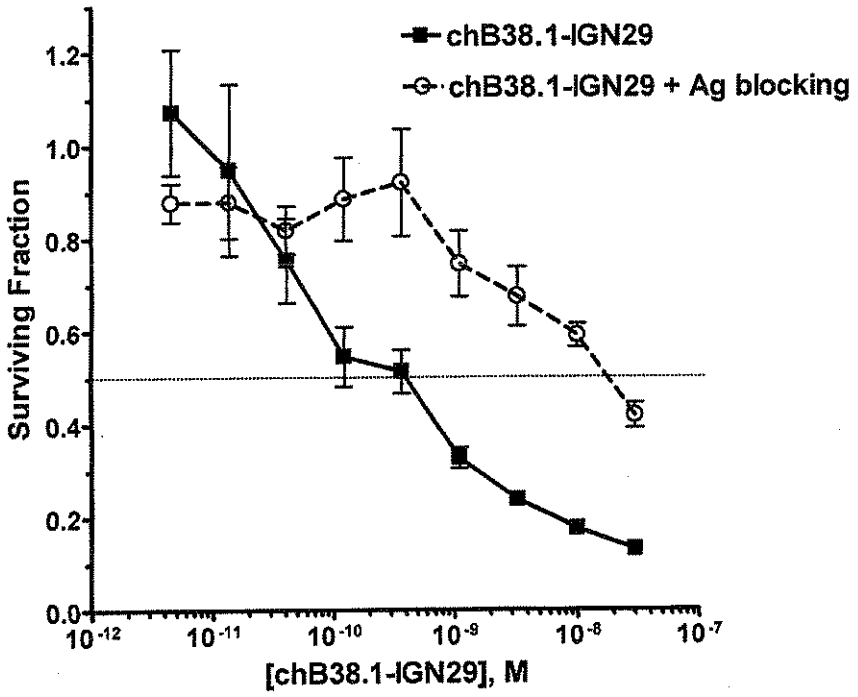


Figure 58. In vivo efficacy of chB38.1-IGN14 in COLO205 tumor bearing nude mice

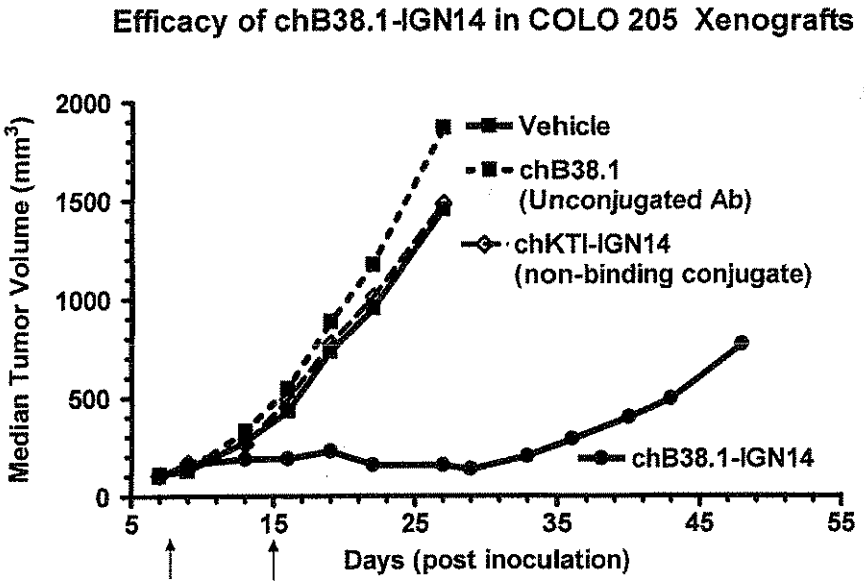


Figure 59. MS analysis of chB38.1-IGN14 conjugate

